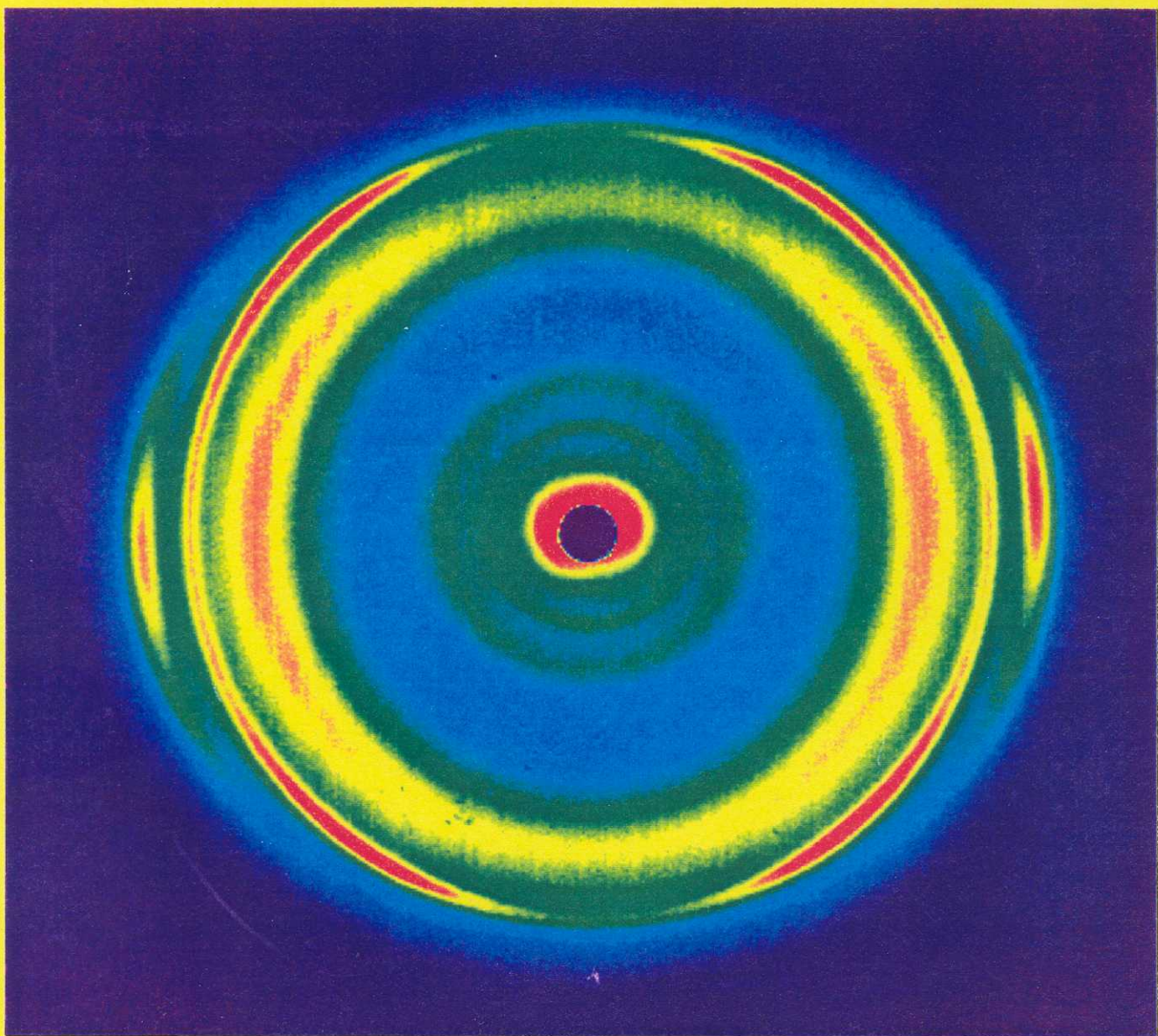


# **THE CCP13 NEWSLETTER**

***Software Development for Fibre Diffraction***



No. 3

DECEMBER 1994

Produced by The Daresbury Laboratory for Collaborative Computational Project 13

---

## **CCP13 OFFICERS 1993/1996**

**CHAIRMAN**  
**NEWSLETTER EDITOR**

DR. JOHN M. SQUIRE  
BIOPHYSICS SECTION  
BLACKETT LABORATORY  
IMPERIAL COLLEGE  
LONDON SW7 2BZ.

Tel: 071 594 7691 FAX: 071 589 0191  
e-mail: j.squire@uk.ac.ac

**SECRETARY**

DR. GEOFF MANT  
DRAL DARESBURY LABORATORY  
WARRINGTON  
CHESHIRE WA4 4AD.

Tel: 0925-603 169 FAX: 0925-603 174  
e-mail: g.r.mant@uk.ac.daresbury

**RESEARCH ASSISTANT**

DR. RICHARD DENNY  
DRAL DARESBURY LABORATORY  
WARRINGTON  
CHESHIRE WA4 4AD.  
(or at Imperial College, as for Dr. Squire)

Tel: 0925-603 636 FAX: 0925-603 174  
e-mail: r.denny@uk.ac.daresbury  
r.denny@uk.ac.ac

---

## **STEERING PANEL**

The current membership is: Dr. John Squire (Chairman; 1996), Dr. Geoff Mant (Secretary; 1996), Dr. Richard Denny (CCP13 'RA'; ex officio), Dr. Mike Ferenczi (1995), Dr. Trevor Forsyth (1995), Dr. Keith Meek (1995), Dr. Manolis Pantos (1996), Dr. Robert Rule (1997), Dr. Tony Ryan (1997).

---

**CONTENTS:**

Chairman's Message	2,3
Cover Illustration	311
Geoff Mant - Report on the 3rd CCP13/NCD Workshop - May 1994	4-6
1994 Poster Prize Abstracts	7
Special Feature: Bruce Fraser - 'Digital Processing of Fibre Diffraction Patterns'	8-11
Richard Denny - 'CCP13 Program Developments'	12-16
Geoff Mant - 'Table of CCP13/NCD Software Available and its Implementation'	17
Bras/ Bordas/ Denny/ Diakun/ Medrano - 'The Fibre Diffraction Pattern of Microtubules'	18-20
Walsh - 'Processing Fibre Diffraction Patterns from Filamentous Bacteriophage using the CCP13 Suite of Software'	21-24
Ryan - 'SAXS Correlation Functions: New Software at Daresbury'	25-30
Simpson/ Shotton/ Forsyth - 'Processing of DNA High-Angle Fibre Diffraction Patterns Using the CCP13 Suite'	31-35
The Fibre Diffraction SIG at the 1995 Montreal ACA Meeting	36
The 1995 CCP13 Workshop	37-39

---

---

## CHAIRMAN'S MESSAGE

The current, third, edition of the annual CCP13 NEWSLETTER is bigger and meatier than ever, reflecting the undoubted success of CCP13. The articles in the Newsletter detail the progress in developing fibre diffraction software in the past year, some ideas about the direction that CCP13 should take in the future, and application of the existing suite to a range of interesting biological and materials science problems. As detailed in the article by Geoff Mant, the 1994 Annual Workshop at Daresbury was a joint meeting of CCP13 and the Non-Crystalline Diffraction community at Daresbury, reflecting the considerable overlap of interests of the two groups. The meeting was very well attended and emphasises the importance of the topic. This year we hope for an even larger audience. Remember that your poster could win a large cash prize (1st Prize - £100; 2nd Prize - £50). There will be bursaries available for students and young scientists. Details of all these are given at the end of the Newsletter.

### Reminder - What is a CCP?

CCP stands for Collaborative Computational Project. CCP13 is currently funded by the UK Biotechnology and Biological Sciences Research Council (BBSRC) via its "Equipment and Facilities" office. It is one of 12 current CCPs. These are:

CCP1	Electronic structure of molecules
CCP2	Continuum states of atoms and molecules
CCP3	Computational studies of surfaces
CCP4	Protein crystallography
CCP5	Computer simulation of condensed phases
CCP6	Heavy particle dynamics
CCP7	Analysis of astronomical spectra
CCP9	Electronic structure of solids
CCP11	Biosequence and structure analysis
CCP12	Novel architecture computers in Fluid Dynamics
CCP13	Fibre diffraction
CCP14	Powder diffraction

Until recently, the general policy on CCPs and the evaluation of their progress has been considered by the CCP Steering Panel, previously chaired by Dr. Julia Goodfellow, Birkbeck College, London, UK. The Steering Panel used to comprise all of the CCP Chairpersons and various observers. However, the restructuring of the Research Councils has meant that some CCPs previously funded by SERC have now been transferred to BBSRC. This includes CCP13, together with CCP4 in protein crystallography and CCP11 on sequence analysis. Most other CCPs are now with EPSRC. Pressure is being applied by CCP chairpersons to re-establish a kind of CCP Steering Panel, but to date this has not happened.

Our current CCP runs to June, 1995. A new application was therefore made to BBSRC for continued funding. Happily this funding has been agreed and the future of CCP13 is secure until the end of September 1998. The new grant will continue the support of Richard Denny as our RA and will provide funds towards Workshops, Newsletter Production and International Interactions. Because of the considerable relevance of CCP13 to the synthetic polymer community, a separate application was submitted to the Materials Board of EPSRC. Unfortunately, although the grant was highly rated and was approved, funding for an extra 'polymer' RA was not provided. Agreed funding was towards the Workshops, Newsletter etc. Since developments on the polymer side are going to be slow without a dedicated pair of 'polymer' hands, further attempts will be made to secure funding for someone to develop 'polymer' software.

---

### Your Contribution

Interested groups or individuals are invited to contact any of the officers of CCP13 to obtain information about CCP13 Workshops, software developments, software standards and so on. Offers of home-written software that could be incorporated into the new CCP13 suite of programs would be much appreciated and will, of course, permanently carry the authors' attribution. Make sure that you are on the CCP13 mailing list and you will be kept informed.

### Newsletter Editorial Policy

Articles for inclusion in the CCP13 Newsletter are welcome by the Editor at any time, but preferably items for the December 1995 issue should arrive before the end of November 1995. It is hoped that the Newsletter will become an Annual 'essential' for Fibre Diffractionists. This is the place to advertise your fibre diffraction or NCD meetings, to report on new software or 'hot' results obtained using the CCP13 Suite and to provide reports of meetings of interest, preferably together with one or two photographs. All technical articles will be scrutinised both for scientific content and presentational style by the Editor (or his nominee) together with at least one other member of the CCP13 Steering Panel. In this way we hope to maintain high standards. Remember that the Newsletter not only goes to other Fibre Diffractionists, but also to various members of the Research Council Secretariats and to other funding agencies.

### International Cooperation

Although these CCPs are UK funded projects, there is a very strong interest in making them international through cooperation with interested scientists in other countries. A natural link for CCP13, for example, exists with the Special Interest Group (SIG) in Fibre Diffraction of the American Crystallographic Association and possibly with some American synchrotron users (CHESS). Others exist with the ESRF at Grenoble and with the Photon Factory in Japan.

---

### COVER PHOTOGRAPH

A single crystal texture from orthorhombic polyethylene.

The WAXS data was taken using an image plate 10 cm from the sample with a helium filled camera. The corresponding SAXS data was also recorded on an image plate at 4.5m with an evacuated camera.

The material is a copolymer of polyvinylcyclohexane (PVCH) and polyethylene (PE). The morphology of the sample is lamella with alternating 100 angstrom layers of semi-crystalline PE and glassy PVCH. The material was oriented under shear prior to crystallisation. The confinement of the PE between glassy layers of PVCH leads to chainfolded crystals oriented parallel to the walls. The X-ray beam is parallel to the lamella and samples the PE crystals along the chain-axis. The simultaneously obtained SAXS pattern (through the hole in the image plate) confirmed the lamella orientation of the block copolymer structure and the semi-crystallinity of the PE.

---

### 3rd Annual CCP13/NCD Workshop

The third annual workshop for the collaborative computational project for fibre diffraction (CCP13) was held in the Tower block seminar room at Daresbury from May 9-11, 1994. This year the meeting was combined with the non-crystalline diffraction (NCD) specialist user group and attracted over 80 participants, twice the number who attended the previous two workshops and reflecting the interest shown in the field. The meeting was partially sponsored by Molecular Simulations and BioSym.

To reflect the joint nature of the workshop a new programme format was devised covering a diversity of topics, including synthetic polymers and liquid crystals, hardware sources and detectors, software developments and biological systems. Each session began with an eminent keynote speaker followed by presentations from specialists in the field. Extending our policy of forging international links, speakers from Australia, France, Austria, Germany and the USA, were invited to give presentations. The talks were complemented by a poster session and commercial exhibition (BioSym and Sun Microsystems).

The meeting opened with a lively presentation by the keynote speaker for the polymer session O.Glatter (Graz), on the desmearing of low angle diffraction patterns, using cubic splines, to reduce the effect of slit width. This was followed by talks from W.Bras (Daresbury) on the combination of simultaneous time resolved techniques small with wide angle scattering (SAX/WAX), including differential scanning calorimetry and Fourier Transform Infra Red. M.J.Elwell (UMIST) described the use of SAX to study the kinetics of flexible polyurethane foam and R.J.Rule (ICI) presented a study on oriented synthetic polymers with a paracrystalline macrolattice. H.F.Gleeson (Manchester) described the application of time resolved X-Ray scattering to the study liquid crystals in the Smectic A phase. A.Mahendrasingham (Keele) described the results of fibre diffraction studies of the structural transitions in organic polymers and the development of a new CCD detector system. A.J.Ryan (UMIST) concluded with a talk on SAX/WAX studies on the polymorphism of polybut-1-ene explaining why bin-bag liners are black.

The hardware session started with C.Reikel (ESRF) providing a description of the facilities at the ESRF for SAX and polymers under high pressure. This was followed by C.C.Wilson (Rutherford Appleton) who described the use of neutron time of flight Laue diffraction and its application to fibres. G.Hall (Imperial College) gave a technical presentation on future detectors constructed from silicon with embedded electronics. N.Fore (Daresbury) described the necessary error corrections that would be required by the new generation of wire chamber detectors. This session was concluded with an overview of the facilities provided by the new Wiggler II station 16.1 on the SRS by E.Towns-Andrews (Daresbury) and the latest improvements in the stopped flow apparatus for studying fast kinetics using time resolved X-Ray diffraction by D.Clarke (Daresbury).

The software developments and results section began with a keynote address on the analysis and simulation of fibre diffraction patterns, emphasising the benefits of converting intensities into a reciprocal space map, by R.D.B.Fraser (Queensland). A.Windle (Cambridge) presented the development of a novel CCD based diffractometer, utilising a three circle goniometer, developed for oriented polymer fibres. The technique relies on the combination of images converted to reciprocal space. D.Svergun (EMBL) described a new approach to interpretation of small angle scattering data to provide shape determination as applied to the 50S ribosomal subunit, using spherical harmonics. W.J.Stroud (Purdue) described the effect of disorder in the crystalline domains of fibres on layer line intensities, showing that there is a gradual transition from Bragg to continuous intensity away from the centre of calculated patterns. A.P.Hammersley (ESRF) described some new developments in a 2D polynomial fitting background subtraction program and its application to the analysis of type I collagen. R.C.Denny (Imperial College & Daresbury) provided an overview of the CCP13 suite of programs including new developments in the LSQINT program with a maximum entropy algorithm. The final presentation of the session was given by A.Stewart (Kings College) who demonstrated with a visual presentation the PC

software used to analyse muscle data recorded at CHESS.

The fourth session on biological systems commenced, with a second presentation by R.D.B.fraser (Queensland), with a review of the molecular structure and cellular organisation of keratin with special emphasis on the outstanding problems in this and collagen. T.Wess (Edinburgh) described modelling the three dimensional structure of type I collagen, both native and heavy atom labelled, to a triclinic unit cell. and K.M.Meek (Open University) showed how the collagen fibrils in scar tissue, from corneal stroma, becomes more ordered but never achieves a normal ordering.

K.C.Holmes (Heidelberg) lead a group of talks on muscle research by describing the structure of F-actin and myosin S1 determined by a combination of protein crystallography and X-Ray fibre diffraction techniques. He also addressed the nature of the actomyosin complex in rigor, by combining the results of cryo-electron microscopy and the crystallographic structures. L.C.Yu (NIH Bethesda) discussed recent results from X-Ray diffraction studies of myosin layer lines in skinned rabbit psoas muscle fibres to determine the effect of temperature and ionic strength on weakly bound cross bridges. Despite a wide variation in the number of attached cross bridges her results showed demonstrated that this did not disrupt the thick filament based arrangement of cross bridges in relaxed muscle. J.M.Squire (Imperial College) described recent developments in the analysis of X-Ray diffraction patterns from fish muscle. By utilising the CCP13 suite of programs, he has made significant progress in modelling the rest state at low resolution, with an aim to modelling the intermediate states to the plateau of tension thereby creating "Muscle the movie".

Finally, V.T.Forsyth (Keele) described the use of X-Ray and neutron fibre diffraction in probing the conformational stability in DNA polymers. M.K.Behan-Martin (Daresbury) discussed the swelling properties and phase behaviour of pharmaceutical ionic and non-ionic creams. J.G.Grossman (Daresbury) described some results of X-Ray solution scattering and modelling on two metalloprotein families, nitrite reductase and transferrin.

B.Fraser and C.Reikel volunteered to be judges for the best poster prize. The First place prize, a cheque for £70, was presented to Ann Willoughby (University of Cambridge), for her poster on "A novel CCD-based polymer fibre X-Ray diffractometer", by chairman J.Squire. Second place was awarded to Mike Elwell along with a cheque for £30. The workshop concluded with a special vote of thanks to Brenda Hamblett for all the hard work and organisation that went into making the whole meeting run smoothly.

Geoff Mant (CCP13 Secretary) Daresbury.

---

**IF YOU ARE A FIBRE DIFFRACTIONIST STUDYING  
SYNTHETIC OR BIOLOGICAL POLYMERS -  
THIS CCP IS FOR YOU -  
PLEASE HELP TO MAKE IT WORK!**

---



Dr. Tony Ryan demonstrates, to 2 delegates during the poster/wine tasting session at the 3rd Annual workshop, the use of correlation functions in the analysis of time resolved small angle X-ray data.

---

## ABSTRACTS OF 1994 PRIZE WINNING POSTERS

---

### **FIRST PRIZE:**

#### **A NOVEL CCD-BASED POLYMER FIBRE X-RAY DIFFRACTOMETER**

**A.M.E. Willoughby, S. Hanna\* & A.H. Windle**

Department of Materials Science and Metallurgy, University of Cambridge,  
Pembroke Street, Cambridge CB2 3QZ & \* now at H.H. Wills Physics Laboratory,  
University of Bristol, Tyndall Avenue, Bristol BS8 1TL.

In X-ray diffraction experiments the diffraction is sampled from  $hkl$  planes whose reciprocal lattice points lie on the surface of the Ewald sphere. For most uniaxially oriented polymers the chain axis lies parallel to the fibre axis. Consequently, in the fibre diffraction transmission photography arrangement most commonly used (with the X-ray beam normal to the length of the fibres), the meridional diffraction cannot theoretically be accessed because of the curvature of the Ewald sphere. Tilting the fibre allows access to the meridian one point at a time, but quantitative interpretation of the results presents difficulties.

A diffractometer based on a scanning X-ray sensitive CCD (charge-coupled device) has been developed for studying highly uniaxially oriented polymer fibres. A three-circle goniometer allows the detector to take snap-shots at different positions in reciprocal space and hence equatorial through to meridional diffraction may be accessed. These images are mapped from detector space to reciprocal space and then combined to form an undistorted composite diffraction pattern which is linear in reciprocal space.

### **SECOND PRIZE:**

#### **FOLLOWING PHASE SEPARATION KINETICS DURING THE FORMATION OF FLEXIBLE POLYURETHANE FOAM USING SYNCHROTRON SAXS**

**Michael J. Elwell, Stephen Mortimer & Anthony J. Ryan**

Manchester Materials Science Centre, UMIST, Grosvenor Street, Manchester M1 7HS.

**& Wim Bras**

EPSRC Daresbury Laboratory, Warrington WA4 4AD.

The kinetics of microphase separation during the processing of flexible polyurethane foam have been investigated. Forced-adiabatic, time-resolved Synchrotron SAXS experiments were employed to probe structure development during processing. Microphase separation was observed to occur at critical conversion of isocyanate functional groups and shown to follow the kinetics associated with spinodal decomposition. The isocyanate conversion at the microphase separation transition (MST) was in good agreement with our previously reported FT-IR results. From the scattering data,  $R(q)$ , the amplification rate of the composition fluctuations was determined. The data have been analysed in terms of a time dependent Ginzburg-Landau model (TDGL). Plots of  $R(q)/q^2$  versus  $q^2$  exhibited a maximum at a finite value of scattering vector ( $q$ ). These observations were in qualitative agreement with the theoretical predictions of the TDGL theory.

---

## Digital Processing of Fibre Diffraction Patterns

R.D.B.Fraser

### Introduction

Fibrous materials generally consist of particles (molecules, filaments or crystallites) which are preferentially oriented parallel to a unique axis termed the fibre axis. Diffraction patterns obtained from such materials contain information about the particles, and also about the material in which they are embedded. This matrix may consist of an amorphous phase of the same composition or may be a distinct structural entity as is the case in many biological specimens. In addition the matrix may contain liquid which also contributes to the observed diffraction pattern.

The extraction of structural information from such patterns is greatly assisted by mapping the observed intensity into reciprocal space to obtain what has been termed the *specimen intensity transform* [1]. This is a type of convolution of the orientation density function of the particles with the cylindrically averaged intensity transform of a single particle. In a perfectly oriented specimen the mapping would provide a central section through the cylindrically averaged intensity transform of the particle, but in practice the intensity at any particular point in the transform is spread out along an arc due to the imperfect alignment of the particles [2].

Reciprocal space mapping of fibre diffraction patterns has been used in studies of both simple polymers and complex biological materials to determine unit cell parameters, to collect intensity data, and to analyse systematic distortion in surface lattices [3-9]. These studies were carried out with programs tailored for specific purposes but recently a suite of programs has been developed which allow the automated extraction of unit cell parameters and structure factor data from patterns which satisfy certain criteria [10]. Many biological specimens however yield patterns that are too complex for this automated procedure to be used and still require individual treatment.

The purpose of this contribution is to direct attention to the potentials of profile analysis and of simulation in dealing with the more complex diffraction patterns, since neither have been fully exploited to date.

### Profile Fitting

The advantages of profile fitting in the extraction of structure factors from single crystal intensity data are well established [11,12] and similar principles are applied in the automated procedure mentioned above [10]. If the expression used to model the profile contains parameters which are directly related the particle dimensions and the distribution of particle directions, the fitted parameters will provide important information about the physical characteristics of the specimen [13].

A major obstacle to the extraction of comprehensive structure factor data from fibre diffraction patterns is the overlapping of reflections due to the cylindrical averaging and this is compounded by the arcing due to the imperfect alignment of the particles. An approach to this problem which has considerable potential depends on the development of a realistic expression for the reflection profile in

terms of parameters directly related to the unit cell dimensions, the shape of the particle, the orientation density function, and any cumulative disorder. A detailed description of this approach and a specific example of its application to the diffraction pattern of *Bombyx Mori* silk fibroin have been given elsewhere [13].

In the case of diffraction patterns with continuous layer lines a technique has been described to deal with the smearing due to disorientation [14] and this procedure can be enhanced by profile fitting with a function which incorporates the effects of finite particle length, and the unit height and unit twist of the helix [15].

## Simulation

An alternative to attempting the extraction of information directly from the specimen intensity transform is to produce a simulated diffraction pattern based on a modelling of the internal structure and spatial organisation of the particles. Visual comparison of the simulated and observed diffraction patterns, using an imaging device such as the Optronics Photowrite, is a valuable aid in identifying discrepancies and suggesting new approaches to modelling. Simulation is particularly useful in the study of multi-component biological materials.

Procedures for calculating the simulated diffraction patterns of fibrous assemblies of particles with 3-dimensionally crystalline structure and of particles with helical symmetry have been described [13, 14]. In the case of a 3-dimensionally crystalline particle three distinct steps are involved:

1. The 3-dimensional distribution of intensity for an infinite particle is calculated with appropriate allowance for random fluctuations in atomic positions, and the influence of solvent on the atomic scattering factors.
2. The simulated intensity distribution across a central section of the cylindrically averaged transform of a single particle is then constructed by incorporating the effects of cumulative disorder within the particle, finite particle dimensions and random azimuthal rotation about the fibre axis.
3. The intensity at each point in the simulated specimen intensity transform is then calculated by numerical integration, with appropriate weighting [2], over an arc of appropriate length in the simulated particle intensity transform.

The procedure used with helical particles is similar except that in Step 1 the cylindrically averaged intensity on each layer line is calculated at intervals of  $R = 1/(2r_{max})$ , where  $r_{max}$  is the radius of an exscribed cylinder enclosing the particle. Intermediate values are interpolated as required. An allowance for random azimuthal rotation is not required in Step 2 since this has already been incorporated in Step 1.

In complex biological materials the particles generally consist of helical molecules or filaments with helical symmetry. These may be packed in a 3-dimensionally crystalline array as in tendon collagen and some muscle fibres, a 2-dimensionally crystalline array as in avian and reptilian hard keratins or in quasi-

hexagonal arrays as in mammalian hard keratin. The steps outlined above can readily be modified to deal with these situations.

Most biological specimens contain appreciable quantities of water and this has a considerable effect on the intensity distribution in the low to medium angle part of the diffraction pattern. The incorporation of procedures for the simulation of this effect is essential in these materials. A simple but effective method is to incorporate the solvent correction in the atomic scattering factor [16]. The low angle region of the diffraction pattern is dominated by the shape function of the particle, which is generally modulated by an inter-particle interference function, and the electron density contrast between the particles and the surrounding medium.

### **Disorder in Biological Materials**

Imperfections in crystalline order in biological materials often play an important role in their biological function and the elucidation of their precise nature is essential for a complete understanding of the structure-function relationship. Transform mapping and simulation provide a valuable tool for studying such disorder. Descriptions of the various types of disorder that have been observed in fibrous structures and treatments of the effects of such disorder on the diffraction pattern are widely scattered throughout the literature and it may be of value to list some of the more important sources of information.

Random displacements of the individual atoms from their idealised positions in the structure can be simulated by the inclusion of an exponential term in the atomic scattering factor [17]. The breadths of reflections and of layer lines are not affected by this type of disorder. In contrast fluctuations in lattice parameters gives rise to an increase in breadth that increases with increasing angle of diffraction [18-22] and measurements of the change in integral breadth in a related series of reflections can be used to estimate values of both the crystallite dimension in a direction perpendicular to the reflecting planes and the statistical fluctuation in the interplanar spacing. In addition to positional disorder, crystalline particles of polymeric materials may be subject to imperfections involving coordinated movements of complete chains [23,24,25] and irregularities in chain direction [25,26,27].

There is abundant evidence from studies of synthetic polypeptides that when helical molecules pack in a regular 3-dimensional array they are subject to systematic distortions due to the fact that the natural helical symmetry of the molecule is incompatible with the crystallographic symmetry [28]. This is an illustration of the concept of quasi-equivalence [29,30] which recognises the possibility that by systematically distorting a regular structure it may be possible to arrive at a structure of lower free energy. These systematic distortions generate long axial periods and layerline 'ghosts' [30-32]. In the complex assemblies encountered in biological materials disorder and systematic distortions are common [5,31-35] and a comparison of observed and simulated patterns provides a valuable means of refining model structures.

### **References**

1. Fraser, R.D.B., MacRae, T.P., Miller, A. & Rowlands, R.J. *J.Appl.Cryst.* 9, 81-94 (1976).

2. Holmes, K.C. & Barrington-Leigh, J. *Acta Cryst.* A30, 635-638 (1974).
3. Meader, D., Atkins, E.D.T., Elder, M., Machin, P.A. & Pickering, M. in *Fiber Diffraction Methods* (eds, A.D.French & K.H.Gardner) ACS Symposium Series 141, 113-138 (1980).
4. Fraser, R.D.B., Macrae,T.P. & Suzuki, E. *J.Mol.Biol.* 108, 435-452 (1976).
5. Fraser, R.D.B. & MacRae, T.P. *Int.J.Biol.Macromol.* 10, 178-184 (1988)
6. Fraser, R.D.B. & MacRae, T.P. *Int.J.Biol.Macromol.* 3, 193-200 (1981).
7. Fraser, R.D.B., MacRae, T.P. & Suzuki, E. *J.Mol.Biol.* 129, 463-481 (1979).
8. Fraser, R.D.B., MacRae, T.P., Miller, A. & Suzuki, E. *J.Mol.Biol.* 167, 497-521 (1983).
9. Fraser, R.D.B., MacRae, T.P. & Miller, A. *J.Mol.Biol.* 193, 115-125 (1987).
10. Denny, R. CCP13 Newsletter 2, 5-8 (1993).
11. Diamond, R. *Acta Cryst.* A25, 43-55 (1969).
12. Ford, G.C. *J. Appl.Cryst.* 7, 555-564 (1974).
13. Fraser, R.D.B., Suzuki, E. & MacRae, T.P. in *Structure of Crystalline Polymers* (ed.I.H.Hall) Elsevier, London , 1-37 (1984).
14. Makowski, L. *J.Appl.Cryst.* 11, 273-283 (1962).
15. Suzuki, E., Fraser, R.D.B., MacRae, T.P. & Rowlands, R.J. in *Fiber Diffraction Methods* (eds, A.D.French & K.H.Gardner) ACS Symposium Series 141, 61-67 (1980).
16. Fraser, R.D.B., MacRae, T.P. & Suzuki, E. *J.Appl.Cryst.* 11, 693-694 (1978).
17. Vainshstein, B.K. *Diffraction of X-Rays by Chain Molecules*, Elsevier, London (1966).
18. Hosemann, R. & Bagchi, S.N. *Direct Analysis of Diffraction by Matter*, North-Holland, Amsterdam (1962).
19. Hosemann, R. & Wilke, W. *Macromol Chem.* 118, 230-249 (1968).
20. Kakudo, M. & Kasai,N. *X-Ray Diffraction by Polymers*, Elsevier, Amsterdam (1972).
21. Hindle, A.M., Johnson, D.J. & Montague, P.E. in *Fiber Diffraction Methods* (eds, A.D.French & K.H.Gardner) ACS Symposium Series 141, 149-182 (1980).
22. Welberry, T.R., Miller, G.H. & Carroll, C.E. *Acta Cryst* A36, 921-929 (1980).
23. Clark, E.S. & Muus, L.T. *Z.Kristallogr.* 17, 108-118 (1962).
24. Tanaka, S. & Naya, S. *J.Phys.Soc.Japan* 26, 982-993 (1969).
25. Arnott, S. in *Fiber Diffraction Methods* (eds, A.D.French & K.H.Gardner) ACS Symposium Series 141, 1-30 (1980).
26. Arnott, S., Dover, S.D. & Elliott, A. *J.Mol.Biol.* 30, 201-208 (1967).
27. Fraser, R.D.B., MacRae, T.P., Parry, D.A.D. & Suzuki, E. *Polymer* 12, 35-56 (1971).
28. Fraser, R.D.B. & MacRae, T.P. *Conformation in Fibrous Proteins*, Academic, New York (1973).
29. Caspar, D.L.D. in *Principles of Biomolecular Organisation* (eds. G.E.W.Wolstenholme & M.O'Connor, Churchill, London, 7 (1966).
30. James, R.W. *The Optical Principles of X-Ray Diffraction*, Bell & Sons, London (1954).
31. Caspar, D.L.D. & Holmes, K.C. *J.Mol.Biol.* 46, 99-133 (1969).
32. Makowski, L. & Caspar, D.L.D. in *The Single Stranded DNA Phages* (eds. D.T.Denhart, D.Dressler & D.S.Ray) Cold Spring Harbor Laboratory, 627-643 (1978).
33. Squire, J.M. in *Fibrous Proteins: Scientific, Industrial and Medical Aspects* (eds D.A.D.Parry & L.K.Creamer) Vol. 1, Academic, London (1979).
34. Holmes, K.C., Tregear, R.T. & Barrington-Leigh, J. *Proc.Roy.Soc.* B207, 13-33 (1980).
35. Luther, K.P. & Squire, J.M. *J.Mol.Biol.* 141, 409-439 (1980).

# CCP13 program developments

Richard Denny  
Imperial College and Daresbury Laboratory

## FIT: Curve and peak fitting

**Introduction** The facility to fit positions, widths and heights of a number of possibly overlapping peaks on top of a variable background can be particularly useful for studying time series of diffraction data. With this type of application in mind, a program, FIT, has been written which uses GHOST graphics and accepts OTOKO-style input. A new version of this program, XFIT, is under development which utilizes a Motif-based graphical user interface and a plotting widget developed at Daresbury.

**Peak shapes** Currently, two peak types are available: Gaussian and Lorentzian. Options can be activated when the pointer is in GHOST window; to change the peak type to Gaussian press  $<\text{g}>$ , to change to Lorentzian, press  $<\text{c}>$ . Voigt and Pearson VII will soon be implemented.

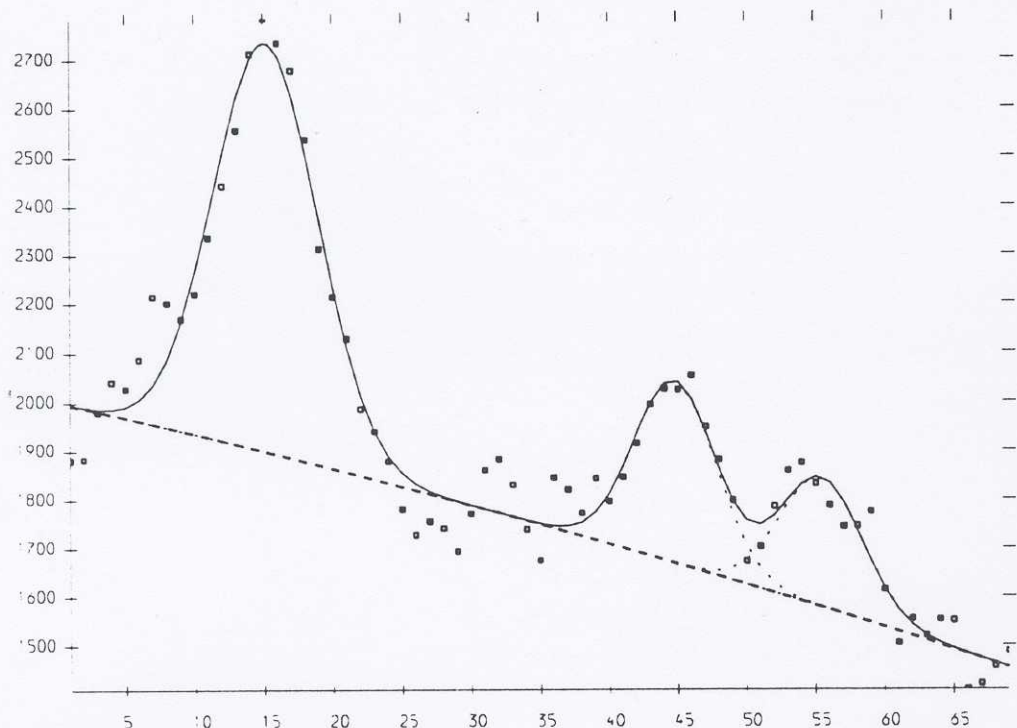
**Background curve** The background can be described by a polynomial of degree  $n$  where  $n \leq 4$ . This is chosen by pressing the appropriate number when the focus is in the GHOST window.

**Selection of initial parameters** The cursor and left mouse button are used to determine the starting point for the non-linear least-squares fitting. The horizontal position of the pointer determining the X-coordinate of the peak and the pointer's height above the base line of the plot determining the width of the peak. When fitting a time series, the initial parameters are determined by the fitted parameters from the previous frame. Alternatively, initial parameters for the whole series can be input from an OTOKO file describing a previous run.

**Constraints** Once the initial parameters have been chosen, it is possible either to set the value of a parameter, thereby removing it from the fit, or the value of a parameter can be constrained to be equal to the value of another parameter, removing a degree of freedom from the fit. For example, one might wish to ensure that the widths of two peaks were equal but that the width was refined along with the other parameters.

**Output** There are three forms of output from FIT, hardcopy output of the GHOST graphics as shown in figure 1, a list of the fitted parameters in an ASCII log file and OTOKO-style output suitable for examining the time-courses of background and peak parameters.

Fig. 1. Result of line fitting with three Gaussians and a cubic background in FIT. The small squares are the data points, the solid line is the total fitted curve and the dashed lines are the background and individual peaks.



## DCV: Main beam deconvolution for small angle diffraction patterns

**Introduction** A large focus presents certain difficulties when processing fibre diffraction patterns. A problem common to all diffraction patterns is that the smearing produced by the focus makes it difficult to identify close-lying diffraction peaks and a loss of information occurs. The smearing out of layerlines in this fashion also causes the disorientation of the fibre pattern to be under-estimated (when the beam is broad in a direction perpendicular to the layerline) which in turn causes a systematic under-estimation of integrated intensity with resolution. Bragg-sampled patterns introduce the further problem of properly Lorentz correcting the data. There are two obvious approaches to this problem: either to attempt to deconvolute the beam profile from the entire diffraction pattern or to convolute the predicted diffraction spot shapes with the beam profile when fitting the pattern. In the program DCV the former approach is adopted in the hope that intensity peaks that may not have been predicted will be made more apparent although this maybe a somewhat optimistic viewpoint.

**Preparation of the image** Regions of the image which are not required for processing (e.g. the backstop, or unexposed areas around the perimeter of the scanned image) can be masked out in the program. Some estimate of the standard deviation of each pixel value is also necessary. This is taken to be dependent only on the pixel value in a relation of the form

$$\sigma_k = \sigma_{min} + \alpha \sqrt{D_k}$$

where  $\sigma_k$  is the standard deviation associated with the  $k^{th}$  pixel and  $D_k$  is the value contained in this pixel. If one does not have this degree of knowledge about the recording medium, the values of  $\sigma_{min}$  and  $\alpha$  can be estimated by fitting a low order polynomial through regions of the image where the intensity varies slowly. Clearly, an image of the undiffracted beam will be required. This is trimmed and normalized by the program for use in the deconvolution process.

**The deconvolution method** The approach taken is similar to that for reconstructing images from blurred pictures. A linear equation is used to relate the blurred image  $\{F_k\}$ , to the ideal, point-focus image  $\{f_j\}$ ,

$$F_k = \sum_j R_{kj} f_j$$

These  $F_k$  can then be compared with the data,  $D_k$  by use of a  $\chi^2$  statistic. The approximations are made that the angular divergence of the beam is small and that the shape of the beam profile does not vary over the image. The first assumption means that the only effect of the beam profile is to provide weighted shifts of the origin of reciprocal space rather than changes in its orientation. The second assumption causes the matrix which describes the beam profile, formed by the  $R_{kj}$  to be of the Toeplitz type which reduces the amount of storage necessary to contain mapping information. This limits the applicability of the program to small angle patterns.

In order to decrease the value of  $\chi^2$  relatively rapidly from the starting value, a conjugate-gradient method is used until  $\chi^2$  is approaching  $M$ , the number of pixels. Henceforth, the maximum entropy algorithm of Skilling & Bryan (1984) is employed to remove structure in the conjugate-gradient solution which is not required by the data.

**Deconvolution of 2-D Gaussian profile from simulated data** In order to test the program, simulated data was produced using the NOFIT option in the program LSQINT. This was then convoluted with a Gaussian profile to produce an image reminiscent of part of a bony fish muscle diffraction pattern recorded on station 2.1 at the SRS. Figure 2 shows these starting patterns along with the solution obtained after 1000 iterations of the conjugate gradient minimization and 500 cycles of the maximum entropy algorithm.

The simulation had no noise added to it, but differences between figure 2(a) and 2(c) can occur due to the accumulation of roundoff errors or the premature termination of the minimization of  $\chi^2$ . So that the a solution could be reached after a reasonable time,  $\sigma_{min}$  was set to 0.5 and  $\alpha$  to 0.025. The presence of "flares" on some of the equatorial reflections despite 500 cycles of entropy maximization is somewhat worrying. A criterion for convergence of the algorithm at the appropriate value of  $\chi^2$  is given by

$$TEST = \frac{1}{2} \left| \frac{\nabla S}{|\nabla S|} - \frac{\nabla \chi^2}{|\nabla \chi^2|} \right|^2 < 0.1$$

for linear problems, where  $S$  is the entropy of the solution relative to some prior distribution (Skilling & Bryan, 1984). The value of  $TEST$  achieved here was 0.117, indicating that yet more maximum entropy cycles are required.

**Conclusion** In principle, as long as one can obtain an accurate representation of the main beam profile and the characteristics of the recording medium are known, then it should be possible to obtain a maximum entropy reconstruction of the desmeared image for small-angle scattering experiments. However, recent attempts with real data have not led to a solution which a desmeared pattern might be expected to look like. In these trials, the main beam profile was recorded after scattering through a blank cell and attenuation through a semi-transparent backstop. A better method may be to use less attenuation and a much shorter exposure time for an otherwise unobstructed main beam as the use of a correct beam profile is critical in obtaining a useful deconvoluted image.

## References

- Skilling J. & Bryan R.K. (1984). *Mon. Not. R. astr. Soc.* **211**, 111–124.

## Beam Profile Deconvolution

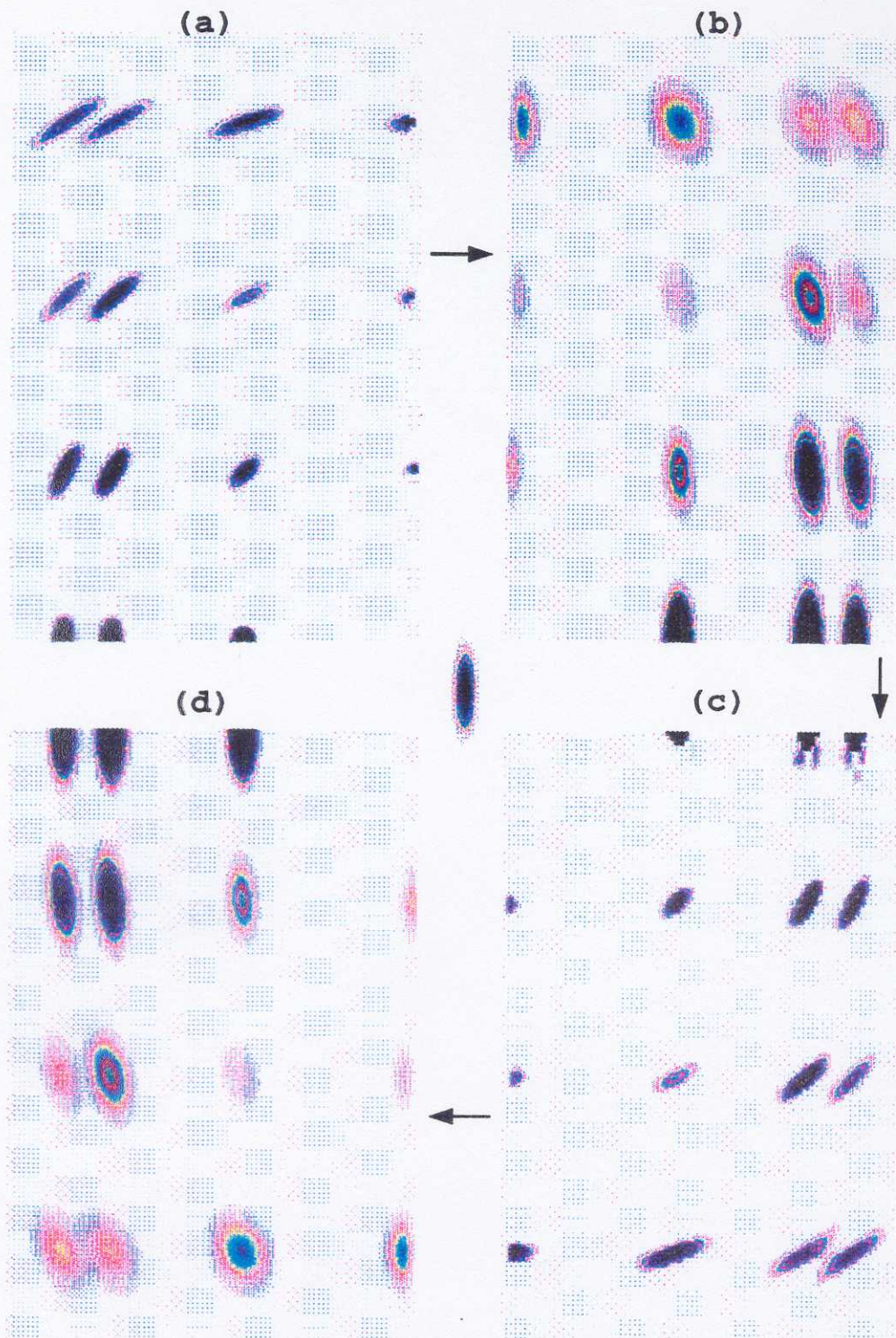


Fig. 2. The simulation used to test the deconvolution program. (a) shows a quadrant of a diffraction pattern simulated with the NOFIT option of LSQINT. (b) is (a) smeared out with the central beam profile. (c) is the output from the deconvolution program and (d) is (c) re-smeared with the beam profile.

---

## SUMMARY OF AVAILABLE CCP13/NCD SOFTWARE

---

Compiled by Dr. Geoff Mant

The following table lists most of the frequently requested DL supported programs, available as executable modules.  
The dates refer to the last software update.

Program	Description	SunOS 4.1.x*	Irix 4 *	HPUX	Ultrix	Irix5.3
xotoko	1-D data manipulation	01/09/94	02/12/93	24/06/92	13/04/92	06/05/94
bsl	2-D data manipulation	16/02/94	02/12/93	27/06/92	13/04/92	06/05/94
xbsl	same as bsl (C version, large arrays)	05/08/94	20/10/94	-	-	05/08/94
v2a	vax to unix data conversion	06/08/91	24/06/92	27/06/92	13/04/92	-
a2v	unix to vax data conversion	19/01/93	02/06/94	-	-	-
otcon	ascii to otoko data conversion	114/06/94	21/06/94	-	-	08/07/94
reconv	otoko to ascii data conversion	05/02/92	-	28/06/92	-	31/10/94
tiff2bsl	image plate to bsl format	25/11/94	-	-	-	-
i2a	ieee to ansi data conversion (DEC only)	n/a	n/a	n/a	09/09/92	n/a
florecc	Image to reciprocal space transformation	17/05/93	-	17/05/93	17/05/93	25/11/94
lsqint	2-D integration & background subtraction	19/09/94	-	19/09/94	19/09/94	25/11/94
fdscale	scaling of intensities	12/06/94	13/06/94	12/01/94	12/01/94	-
fd2bsl	conversion of intensities to BSL format	05/08/93	27/04/94	05/08/93	05/08/93	-
fix	view fibre patterns and get parameters	14/10/94	-	-	-	25/11/94
u2v.exe	VMS record conversion (VMS only)	n/a	n/a	n/a	n/a	n/a

Implementations for Solaris 2.4 should be available soon. SunOS & Irix4 versions will remain frozen  
n/a is not applicable.

## The fibre diffraction pattern of microtubules.

Wim Bras, Joan Bordas, Richard Denny, Greg Diakun, Javier Medrano

Microtubules are long flexible macromolecular assemblies which constitute, among else, part of the cyto-skeleton and the mitotic spindle. A microtubule is a hollow cylindrical structure of 30 nm diameter and a wall thickness of 8 nm. The microtubule wall consists of tubulin heterodimers, which are assembled in a head to tail fashion, into the so called protofilaments. Thirteen protofilaments connect laterally to form the hollow microtubule. The protofilaments are slightly staggered with respect to each other. See figure 1.

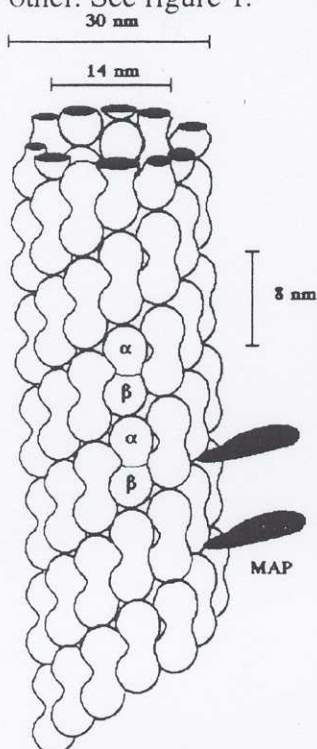


*Figure 1 Schematic drawing of an assembled microtubule. The  $\alpha$ - $\beta$  heterodimer is indicated as well as the two microtubule associated proteins which stick out of the microtubule wall and are thought to be essential for the functioning of the microtubules in the cell.*

Several attempts to obtain fibre diffraction patterns from microtubules have been reported. Unfortunately the results are of low quality or the degree of hydration is disputable. The most successful method for orienting the samples so far has been to centrifuge them at high speeds over extended periods (24 hours). A possible alternative method might be to shear the sample material. Oriented samples have indeed been produced in this way but the uniform shear field essential for the orientation of the samples could only be obtained with a Couette type of shear cell which renders this method unusable for the preparation of X-ray fibre diffraction samples.

We have developed an alternative orientation method. By assembling the samples in a strong magnetic field ( $>7$  Tesla) it was shown to be possible to obtain a high degree of orientation. It is thought that this is possible due to the fact that the small diamagnetic moment of the  $\alpha$ -helical components of the tubulin heterodimer has a net component along the dimer axis. When the microtubules assemble these diamagnetic moments will be vectorially added so that a larger total diamagnetic moment is created. The success of this method is heavily dependent on the buffer conditions, the protein concentration and the strength of the magnetic field. It is only shown to be possible to obtain good orientation in solutions of up to 9 mg/ml in a heavily scattering, glycerol assembly buffer. Experimental difficulties are the high radiation sensitivity of the samples and the relatively low concentration, which means that the data obtained on several samples, over several days, have to be averaged. This is a severe test for the stability of the detector systems and it has been shown that the data collected suffers more from drift in the detector performance than from low statistical accuracy. The fibre diffraction pattern obtained in this way shows that there still is a considerable angular spread in the microtubule axes. See figure 2. A fortunate side effect of the relatively large arcing of the diffraction features is that the errors introduced by detector drifts are, to a large extent, averaged out.

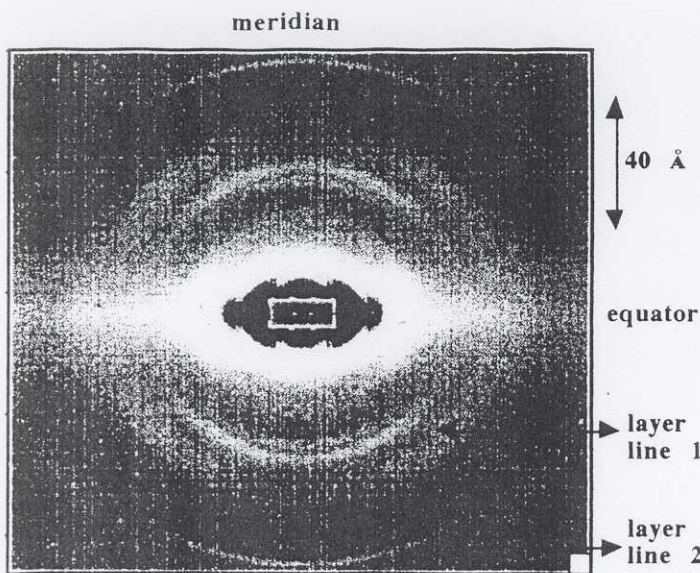


Figure 2 The fibre diffraction pattern of pure microtubules assembled in a 9 Tesla field. The data is the average of data collected on 8 individual samples. Total data collection time 3.5 hours, collected over a period of three days. Average protein concentration 7.5 mg/ml.

In order to obtain reliable diffraction information it was necessary to correct the diffraction pattern for the effects of the angular spread. To achieve this the diffraction pattern was first remapped onto the diffraction sphere using the program FTOREC. After this transformation was applied the program LSQINT was used to calculate what the effect was from the angular spread on the diffraction features. This enabled us to determine what the diffraction intensities on the equatorial axis and the first layer line were. An important result from this was that some intensitiy maxima, observed in the solution scattering pattern, could be shown to be due to higher order repeats from Bessel functions contributing to the equator instead of being due to the first layer line bessel function contributions. These higher orders have not been seen before (by other authors) and are not clearly visible in the uncorrected pattern. See figure 3.

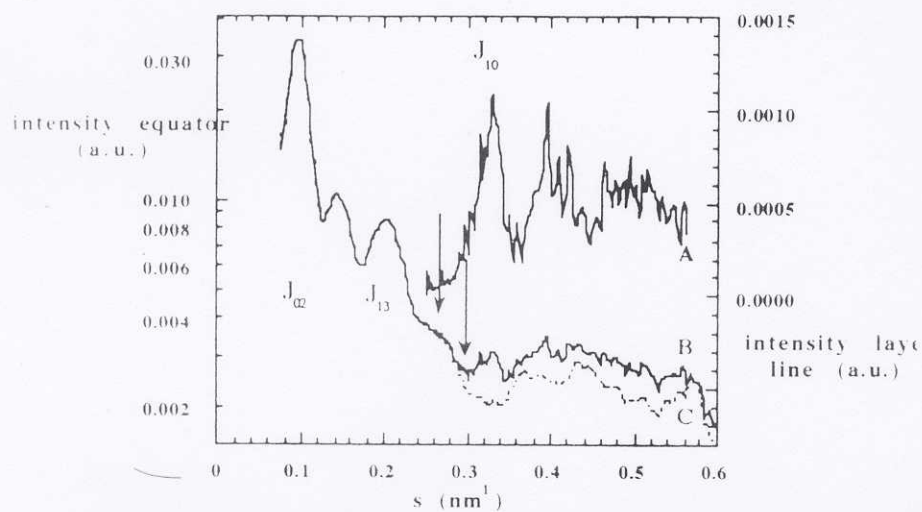
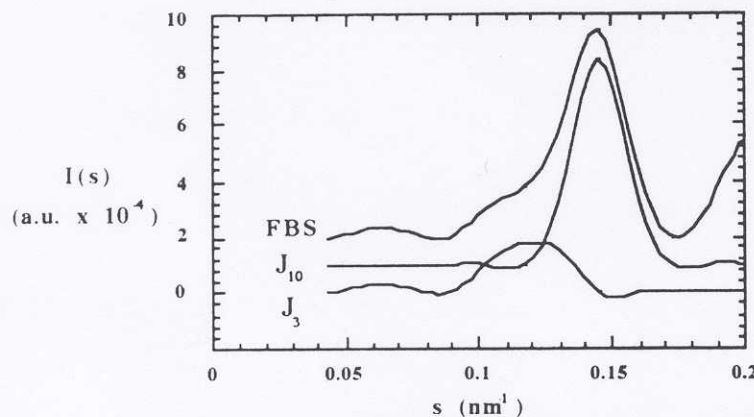


Figure 3 Diffraction intensities on the equator (C), the projection of the first layer line onto the equator (A) and the simulated solution scattering pattern (B). The position of the  $J_3$  contributions, which are clearly dominated by the higher order maxima of the equator, are indicated with the arrows.

However, due to the angular spread, the program LSQINT interprets data near the meridional axis, on the first layer line as true meridional reflections. Since the microtubules have a helical symmetry this is not realistic. Therefore we investigated

the possibility of treating the first layer line with an intelligent procedure of Fourier-Bessel smoothing. By forcing the fitting procedures to obey the rules of helical diffraction it was possible to resolve individual  $J_3$  Bessel function contributions arising from the inside as well as outside wall of the microtubule (see Fig. 4). The fact that the microtubule wall dimensions calculated from these  $J_3$  Bessel functions are in good agreement with the dimensions determined by alternative methods reinforces the belief that the procedure is valid.



*Figure 4 Fourier-Bessel smoothed near meridional first layer line diffraction intensity. In the original data set the two  $J_3$  functions arising from respectively the outside and the inside microtubule wall could not be resolved in the unprocessed data.*

We have shown that by intelligent use of CCP13 software it is possible to extend the possibilities of data analysis, even with rather disoriented specimens such as microtubules, in an apparently sensible way.

## Processing fibre diffraction patterns from filamentous bacteriophage using the CCP13 suite of software

Liam C. Welsh

Cavendish Laboratory, University of Cambridge, Madingley Road, Cambridge.

The purpose of this article is to give a 'users' view of at least some of the CCP13 suite of software, and by illustrating how the suite is used in one particular line of work to give those who may not have used the suite some idea of what it can do.

The filamentous bacteriophages are flexible filaments about 60Å in diameter and 1-2μm long, with a shell of  $\alpha$ -helical protein subunits surrounding a core of DNA. Fibre diffraction studies on the structure of filamentous bacteriophage first started about 30 years ago<sup>1</sup>. One of the projects we are currently working on is the refinement of a model<sup>2</sup> of the Class I, fd strain, of filamentous bacteriophage against a 3Å fibre diffraction data set. A typical diffraction pattern from a magnetically aligned fibre of the Y21M mutant of fd<sup>2</sup> is shown in Fig 1. This pattern shows a mixture of Bragg sampled and continuous intensity on the equator and first two layer-lines, and continuous intensity elsewhere. If the low angle data in the regions of the pattern which exhibit Bragg sampling are required, then our approach has been to prepare a gel from an oriented fibre by adding water to a fibre in a capillary<sup>3</sup>. The inter-particle spacing is then large enough so that only continuous intensity is observed on the fibre pattern, however the increased disorientation in such a specimen means that only the low resolution data can be extracted from these patterns. These gel data are merged with the wide angle fibre data to form a complete data set.

We have been using the CCP13 suite of software in its current form to process our data for the past year. During this time we have collected data on film, Molecular Dynamics image plates, and on a MAR research image plate on station 7.2 of the SRS Daresbury. The recorded image of the diffraction pattern is first converted into BSL format (the CCP13 standard image format) using one of two programs: CONV, for scanned film or MAR data or TIFF2BSL, for MD data.

The next step is to calibrate the image using the program FIX. This program is useful in a number of ways. Firstly it allows the user to determine the specimen to film distance from a powder ring, the image centre, the image rotation, and the specimen tilt. Secondly once these parameters have been determined the reciprocal space co-ordinates of any Bragg reflexions may be measured. Furthermore we use FIX at each stage of the processing of the fibre data to simply display images output from other programs in the suite, as FIX permits up to ten images to be displayed simultaneously using either greyscale or false colour, and the contents of any window may be written out as a colour

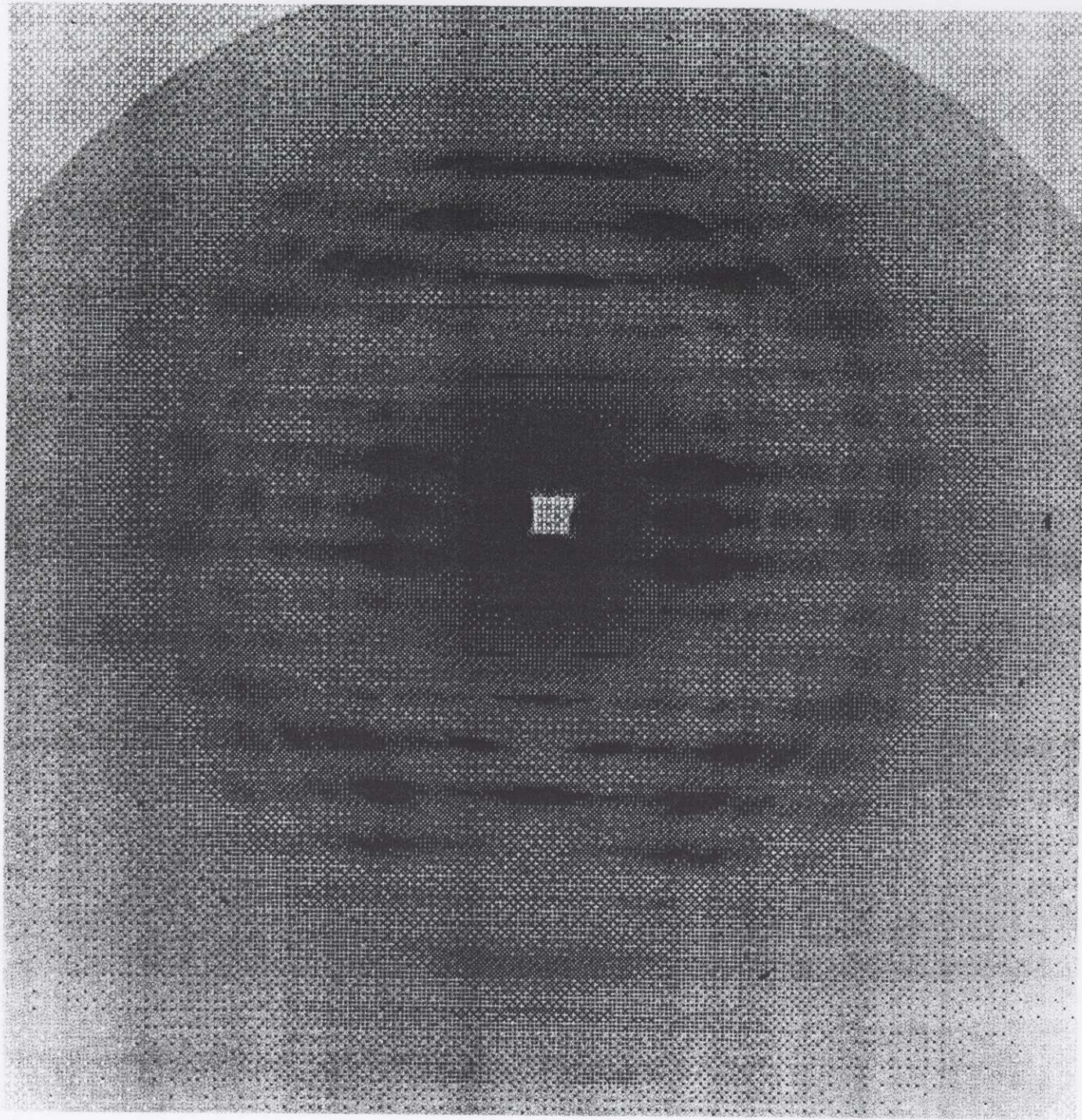


Figure 1.

X-ray diffraction pattern of the Y21M mutant of filamentous bacteriophage fd. The specimen was a fibre made by drying a concentrated solution of the phage in the bore of a 7T magnet. The diffraction pattern was recorded on film at station 7.2 of the SRS Daresbury using a wavelength of  $1.488\text{\AA}$ . The fibre axis is vertical and the Si powder ring is at  $3.14\text{\AA}$ .

postscript file. Alternatively the general image manipulation program **BSL** can be used to generate a contour plot of an image, and a utility, **GRID2PS**, used to produce hard copy. **FIX** also allows a user to look at the variation of the intensity in an image along a user defined line, and this feature has been useful in checking the integrated layer-line intensities that are finally obtained at the end of the data extraction process. **BSL** may also be used for this purpose.

Once a fibre diffraction image has been calibrated it can be mapped from film space to reciprocal space using **FTOREC**<sup>4</sup>, where it will be quadrant averaged by default. However if this is not desired the user may mask out any portion of the image using **BSL** prior to processing with **FTOREC**. A useful feature in **FTOREC** is the option to output an image corresponding to the standard deviations of the values in the reciprocal space bins, as this gives a good check on the accuracy of the calibration obtained in **FIX**. If for some reason the calibration is slightly incorrect then the only solution at the moment is to calibrate the image using **FIX** once more. However there are plans to implement some sort of refinement procedure for the image calibration parameters in **FTOREC** in the future.

After a satisfactory reciprocal space image has been obtained one may proceed to subtract a background from the image and fit the diffracted intensity using **LSQINT**<sup>4</sup>. This program can fit Bragg sampled data or continuous data, but not both together in a single image. In most of the recent work with filamentous bacteriophage we have been concerned with extracting only the continuous intensity from our diffraction patterns, and so we have used the maximum entropy peak fitting option in **LSQINT** (as opposed to the least squares option)<sup>4</sup>. This has proved to be quite straightforward to use and has yielded good data fairly quickly.

The ability of **LSQINT** to refine the unit cell and profile (disorientation and particle coherence length etc.) parameters together during the fitting is useful, but obviously can be slow if an attempt to refine many parameters together is made. The best policy is to get as close to the true profile parameters as possible by eye using the 'nosfit' option (where only the calculated profiles are output and no intensity fitting takes place), prior to calculating a fit to the data. Of the four background subtraction methods available in **LSQINT**<sup>4</sup> the most satisfactory for our work seems to be the Paul Langan roving window method. This method seems very robust and has the advantage that it does not require any information about the sampling point profiles and so can be used reliably even if one is not yet entirely happy with the estimates of the profile parameters. Alternatively it is perfectly possible for a user to remove a background from an image with some other program, if desired, before processing with **LSQINT**, and there are plans to introduce an interactive background subtraction facility into **FIX**.

The quality of a given fit to an **FTOREC** image may be judged from several different data output by **LSQINT**. Firstly an image corresponding to the calculated background is output and this can be inspected using **FIX**, a second image is also output consisting of the fitted intensity profiles and background image together, and this may be compared using **FIX** with the input **FTOREC** image. **LSQINT** also

calculates an R-factor for the fit as well as such quantities as the sum of the background and fitted peak pixels and the sum of the observed pixels minus background. Our experience suggests that the R-factor for a satisfactory fit will be somewhere in the region of 0.1 to 0.4 depending on the number of profiles being fitted. The R-factor is calculated over the entire FTOREC input image regardless of whether LSQINT is fitting the whole image or not, so large R-factors can arise if a portion of an image is not being fitted for some reason. Lastly the output  $F(hkl)$  or  $F(RI)$  (for continuous data) may be plotted and compared with line plots from the raw image data in FIX.

The only difficulty encountered in LSQINT has been with over fitting the input image, resulting in noisy or even spurious intensity profiles. However this problem can be circumvented by using the 'sigma' option for specifying the standard deviations of the input image pixel values, and so weighting the fit. Since the standard deviations are not usually known they are calculated from the pixel values using:  $sd = \min + fact * \sqrt{I}$ , where min and fact are user defined. The choice of these parameters involves some guesswork, but in practice it has been possible to find values for these parameters which result in an accurate fit to the data and in smooth intensity profiles.

A further feature of LSQINT which has proved very useful in our work is the ability to easily simulate a fibre pattern from a set of calculated  $F(hkl)$  or  $F(RI)$  (for continuous intensity). The user must supply an ASCII text file with columns containing  $h, k, l, R$ , and  $I$ , then LSQINT will output an image of a single quadrant of the simulated pattern for given lattice and smearing parameters. One may produce a full fibre pattern using the program EXPAND, which takes a BSL format image of a quadrant of a fibre pattern and mirrors it about the equator and meridian, as it sometimes easier to see what is happening on the equator from a full pattern. Finally it should be noted that LSQINT can deal with diffraction patterns from fibres in which the  $c$  axis of the crystallites is not parallel with the fibre axis, as in fibres of the synthetic polymer PET<sup>5</sup>, and in fibres of wild-type fd filamentous bacteriophage<sup>2</sup>.

So, the CCP13 suite as it stands, allows one to rapidly extract quantitative intensity data from a fibre pattern obtained from most commonly used area detectors, and also to simulate a fibre pattern from a set of calculated  $F(hkl)$ . Currently, what a user does with the set of observed  $F(hkl)$  thus obtained or how a user calculates a set of  $F(hkl)$  from a model, is outside of the scope of the software suite.

## References

- D. A. Marvin (1966) J. Mol. Biol. **15**, 8.
- D. A. Marvin, R. D. Hale, C. Nave & M. Helmer Citterich (1994) J. Mol. Biol. **235**, 260.
- M. F. Symmons, L. C. Welsh, C. Nave, D. A. Marvin & R. N. Perham (1995) J. Mol. Biol. **245**, 86.
- R. Denny (1993) The CCP13 Newsletter No. 2
- H. Tadokoro (1979) Structure of Crystalline Polymers p162. John Wiley & Sons, Inc.

# SAXS CORRELATION FUNCTIONS : NEW SOFTWARE AT DARESBURY

Anthony J Ryan

Manchester Materials Science Centre, UMIST, Grosvenor Street, Manchester M1 7HS  
and DRAL Daresbury Laboratory, Warrington, WA4 4AD.  
(email : tony.ryan@umist.ac.uk)

## 1. Introduction

A set of programs for performing correlation function analysis of one dimensional SAXS patterns have recently been written by Tom Nye (an undergraduate in the Applied Mathematics Department at Cambridge) who worked for me for a month in the summer. This report is based on the instruction manual he wrote to accompany the programs (which must be the first test programs I have ever received with decent documentation!). The programs are based on the SUN network at Daresbury, but have also been copied across and are working on a SUN at UMIST. From a given SAXS image they calculate the one and three dimensional correlation functions, and analyse the one dimensional function in terms of an ideal lamellar morphology<sup>1</sup>. The two correlation functions (called  $\Gamma_1$  and  $\Gamma_3$  respectively) are essentially Fourier transforms of the given one dimensional SAXS curve<sup>2</sup>. They are often interpreted in terms of an imaginary rod moving through the structure of the material from which the SAXS curve was obtained.  $\Gamma_1(r)$  is the probability that a rod of length  $r$  moving through the material has equal electron densities at either end. Hence a frequently occurring spacing within a structure shows up as a peak in the one dimensional correlation function. The difference between  $\Gamma_1$  and  $\Gamma_3$  lies in the assumptions made about the experimental material. The interpretation of  $\Gamma_1$  assumes that, within the SAXS length scale, spacings occur along one fixed axis, but that the axis assumes all possible directions throughout the material. Similarly,  $\Gamma_3$  assumes that spacings can occur in all three dimensions within the SAXS length scale.

The task of calculating and interpreting the correlation functions can be broken down into three logical parts:

- Extrapolation of the experimental SAXS curve to  $q=\infty$  and  $q=0$ .

This is a mathematical requirement for the Fourier transform to be performed. Any SAXS experiment gives a finite number of intensity values at finite values of  $q$  necessitating this extrapolation and a numerical integration to calculate the transforms. It should be stressed that extrapolation to  $q=\infty$  (tail fitting) is the most problematic task of correlation function analysis, and can greatly influence results obtained; the programmes are called `tailfit` and `tailjoin..`

- Fourier transformation of the extrapolated data.

$\Gamma_1$  is based on a cosine Fourier transform, while  $\Gamma_3$  is based on a sine transform. The two functions are related by a simple expression<sup>2</sup>. The program `transform` performs the Fourier transformations, and is relatively simple. It can also re-transform  $\Gamma_1$  back into a smoothed copy of the extrapolated data.

- Interpretation of  $\Gamma_1$  based on an ideal lamellar morphology.

A model is required for the interpretation of features of  $\Gamma_1$  to be possible. The program `extract` performs this analysis. Note that no interpretation of  $\Gamma_3$  is performed.

Correlation functions are extremely valuable tools in the interpretation of one dimensional SAXS patterns, particularly those for which features are either weak or obscured (for example shoulders). However, as with any involved method of analysis, care should be taken to ensure results are genuine and meaningful.

## 2. Program structure.

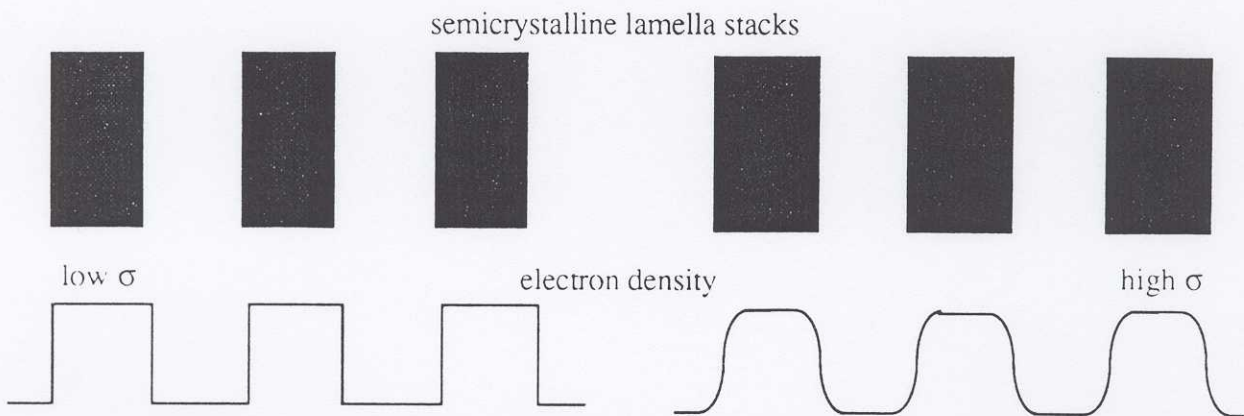
The programs were written in a modular form to enable the code to be incorporated in the GUI version of otoko due over the next few years. The programs also had to be transportable between systems. Each program is run from a UNIX shell script. The shell script runs each of the programs in turn, and also controls graphics output. The programming behind this is complicated, but was written to ease transport of the programs. To plot a graph, a program creates otoko format files containing the data, and a set of shell scripts. The shell scripts run otoko and force it to plot the data contained in the files just created. This may seem an unnecessarily complicated way of producing plots, but it can be used on any system that supports the Xwindows version of otoko, and in general works seamlessly. The programs require an intensity file corrected for the transmission, background and detector response and a q-axis from otoko

## 3. Programs

Tailfit fits either a Porod<sup>3</sup> or sigmoid<sup>4</sup> profile to the tail of the intensity data. It then passes the fit parameters to tailjoin for extrapolation of the data to  $q=\infty$ . The sigmoid profile should generally be used. It uses an intensity profile of the form:

$$I(q) = B + \frac{Ke^{\sigma^2 q^2}}{q^4}$$

where  $B$  is a Bonart thermal background,  $K$  is the Porod constant, and  $\sigma$  describes the electron density profile at the interface between crystalline and amorphous sections



The parameter  $\sigma$  is in Å, and is a measure of the width of the distribution that gives rise to the sigmoid electron density profile. Fitting with a sigmoid profile is a non-linear problem, and requires a robust fitting algorithm: a Levenburg-Marquart method<sup>5</sup> is used.

The Porod tail profile has the form

$$I(q) = B + \frac{K}{q^4}$$

and usually gives poor quality correlation functions, it is included for completeness. However, if a Porod profile is used, a greater number of structural parameters can be extracted, including interface surface to volume ratios and the Porod characteristic chord length. Fitting becomes a linear problem, and so can be less problematic than fitting to a sigmoid profile.

The most important parameters controlled by the user are those concerning which data are used for the tail fitting. If time-resolved data is being analysed, the user can input different channel numbers for each frame. Choosing limits can be difficult, and some experimentation may be required. As a general rule, the start channel should have a  $q$  value about twice that at which any peak occurred in the intensity data. The end channel should be as large as possible, but should avoid any detector noise.

Since the experimental data is extrapolated to very high  $q$ , the majority of the data used in the Fourier transform comes from the tail fit. It's therefore very important to check that the tail fit is good. The tail affects points on the correlation function at low values of  $r$  (real space coordinate) to the greatest extent, but these points are the most important in the extraction of ideal lamellar morphology parameters. Hence the results from an analysis session depend greatly on the tail fit. Choosing channel limits is a payoff between using as many points as possible to ensure a good fit, but wanting to keep as many points as possible from your experimental data in the extrapolated data that is passed to the Fourier transform. A noisy tail on the experimental data will result in poor tail fits, possibly making correlation function analysis impossible.

Tailjoin extrapolates the experimental data back to  $q=0$  using a Guinier model<sup>6</sup>. It then creates otoko files containing intensities from  $q=0$  to beyond  $q=0.6$  using the parameters found by tailfit. The intensity profile used by the Guinier model has the form:

$$I(q) = Ae^{Bq^2}$$

where  $B$  is negative. The Guinier model assumes the small angle scattering arises from particles and the parameter  $B$  is related to the radius of gyration of those particles. This obviously has dubious applicability to polymer systems. However, the correlation function is affected by the Guinier back-extrapolation to the greatest extent at large values of  $r$ , and so the back-extrapolation only has a small effect on the analysis. The Guinier profile is fitted to the first few genuine scattering points after the beamstop. If your experimental data does not contain an upturn in intensity at low  $q$ , back extrapolation may fail. As an alternative to the Guinier profile, a Vonk profile can also be used

Due to the nature of the tail fitting, the join between experimental data and data in the calculated tail usually involves a step that could cause ripples in the correlation function. Hence this join is smoothed using a Savitzky-Golay<sup>5</sup> smoothing algorithm that smoothes the joins without greatly altering higher moments of the data. The point in  $q$  to which extrapolation is performed affects the correlation functions, particularly if it is too small. The value of  $q=0.6$  used by the programs was decided on after experimentation, and gives smooth correlation functions without loss of speed. The lower the truncation point is, the rougher the correlation functions, while the higher the truncation point is, the slower the transform. A truncation point of  $q=0.6$  corresponds to fluctuations in the correlation functions of about 10 Å. These are usually not observable.

Transform performs the integration's necessary to calculate the correlation functions and second moment of the data. It also has the capability of re-transforming  $\Gamma_1$  back into a scattering curve.  $\Gamma_1$  and  $\Gamma_3$  are given by:

$$\begin{aligned}\Gamma_1(r) &= \frac{1}{Q} \int_0^\infty I(q) q^2 \cos(qr) dq \\ \Gamma_3(r) &= \frac{1}{Q} \int_0^\infty I(q) q^2 \left( \frac{\sin(qr)}{qr} \right) dq\end{aligned}$$

where  $I(q)$  is the scattering intensity and  $Q$  is the second moment or invariant given by

$$Q = \int_0^\infty I(q) q^2 dq$$

Hence  $\Gamma_1(0) = \Gamma_3(0) = 1$ . Notice that every point in the extrapolated dataset will be used to calculate each point on the correlation functions, leading to a smooth correlation function. Of course, the integration is numerical and is only performed up to  $q=0.6$  as discussed in the last section. Together with the fluctuations introduced by this truncation, fluctuations are also introduced into the correlation functions by the finite gap between points in the extrapolated

dataset - we don't have intensity as a continuous function of  $q$ . As a final comment, note that the numerical integration takes the form of a trapezium approximation.

*Extract* interprets  $\Gamma_1$  in terms of an ideal lamellar morphology, and extracts structural parameters. The program also displays the results of calculating the moments of the experimental SAXS curve, and Porod results. If tail fitting was performed using a Porod instead of a sigmoid profile, a more detailed Porod analysis is performed. The program first decides whether a lamellar interpretation can be applied. It searches for the first local minimum with a negative  $\Gamma_1$  coordinate and the first local maximum with a positive  $\Gamma_1$  coordinate. If these cannot be found, extraction of the lamella structural parameters is abandoned (for that particular frame). If these features are found extraction can be performed, and will employ these two features. Note these criteria very carefully: local minima above the abscissa will be ignored and not used in the calculation of structural parameters. Similarly, local maxima below the abscissa will not be used in the calculation of structural parameters. Indeed, the interpretation of any one dimensional correlation function deviating from the ideal lamellar model is not yet properly understood.

A diagram of the one dimensional correlation function from an real lamellar morphology is given later. It is essentially a damped Patterson function and consists of a gradually decaying oscillation, with an initial linear section at low values of  $r$ . Structural parameters are derived from the positions of the first local minimum and local maximum, and the position and gradient of the linear section, the complete set of parameters extracted are given below.

Parameter	Symbol	Measurement
Long period	$L_p$	As in diagram
Bulk crystallinity	$\phi$	$\Gamma_{\min} / (\Gamma_{\min} + \Gamma^*)$
Shortest block thickness	$L_c$	As in diagram
Longest block thickness	$L_a$	$L_p - L_c$
Local crystallinity	$V_1$	$L_c / L_p$
Average core thickness	$D_0$	As in diagram
Average interface thickness	$D_{tr}$	As in diagram
Polydispersity		$\Gamma_{\min} / \Gamma_{\max}$
Electron density contrast	$\Delta\rho$	$Q / \phi (1-\phi)$
Specific inner surface		$2\phi / L_c$
Non-ideality		$(L_p - L_p^*)^2 / L_p^2$

Most of these parameters are given in reference<sup>1</sup>. The polydispersity measurement was suggested to Tom by Guy Eeckhaut of ICI. The problem of determining  $D_{tr}$  and  $D_0$  has not been straightforward. Algorithms have been developed with consistency as a priority, so that even if the structural interpretation of these parameters is dubious, the line they specify gives consistent values to the bulk crystallinity, hard block thickness and so on. This has not been an easy task, made harder by the fact that poor tail fits radically alter the appearance of  $\Gamma_1$  at low  $r$ .

*Extract* is an exception to the rule that all user input occurs in `tailinput`, should the lamella model fail then the user is requested to input values of the crystallinity, and some control over the initial straight-line portion is also possible. If a Porod tail fit has been used then *extract* will perform the surface to volume analysis.

## 7. Using the program on real data

An example of a SAXS pattern from a time resolved experiment on polypropylene is given below. The data were collected in SAXS/WAXS/DSC mode on beamline 8.2 with a time resolution of 6s. Note that the data are still quite noisy but the tail joins are good as indicated by the smooth  $\Gamma_1$  which turns over at  $r > 0$ . There is good agreement between the long-

spacing from the correlation function and that obtained by applying Braggs Law to the peak in the Lorentz corrected intensity. In this experiment 256 frames were taken during melting and recrystallisation and running the program on the full set took  $\approx$  45 minutes on a SUN SPARC IPX. The correlation function analysis proved invaluable in analysing the lamella thickness and local crystallinity during melting and recrystallisation and given crucial insights into these processes<sup>7</sup>.

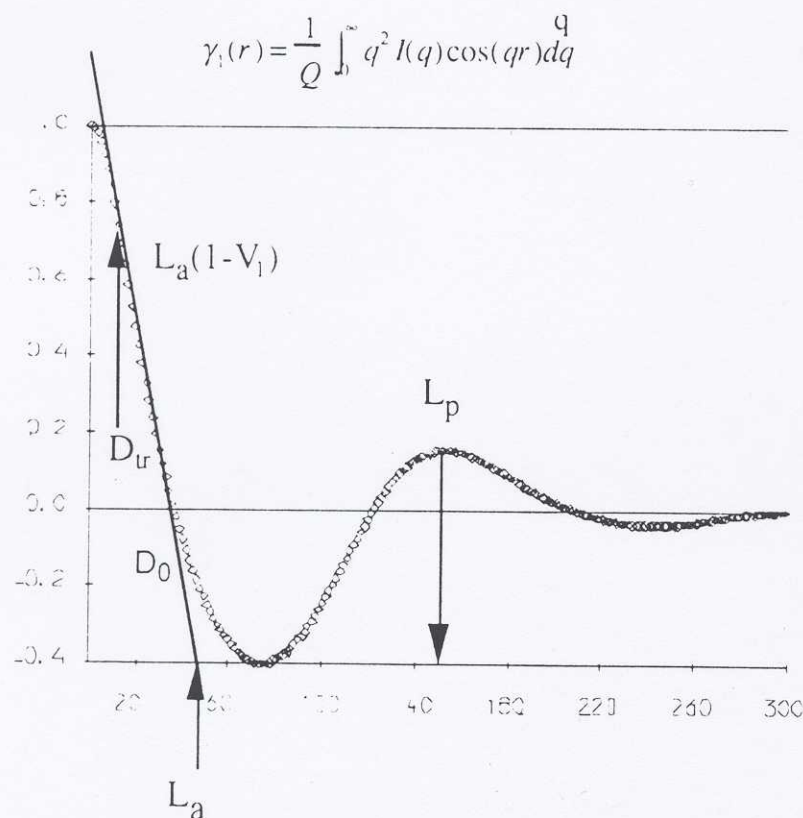
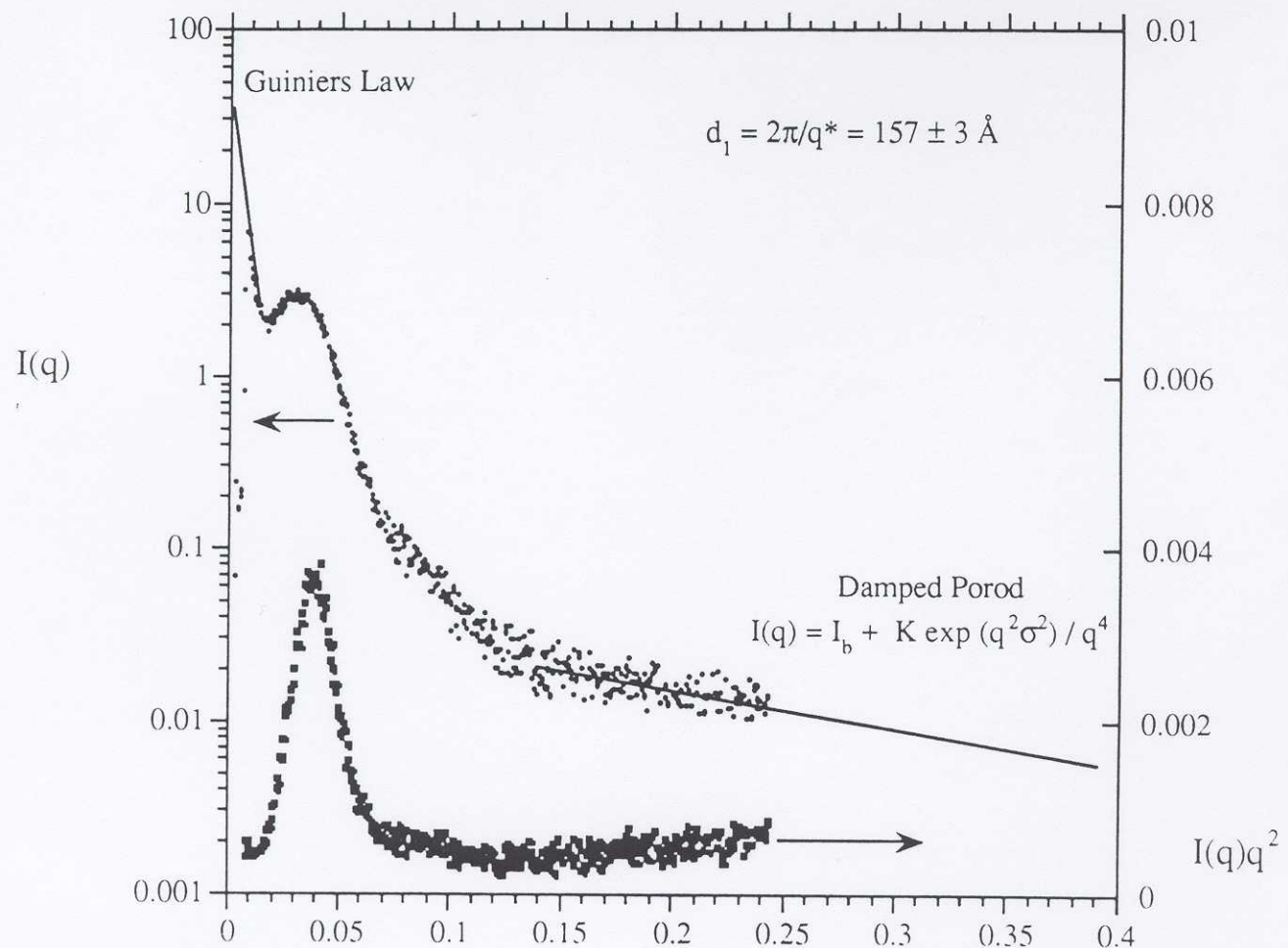
### 8. Conclusion and recommendations.

The crux of the problem lies in tail fitting. The Fourier transformation of data seems to be error free, and artefacts introduced by the extrapolation, while certainly present, don't often affect the correlation functions noticeably. But the appearance of the correlation functions, and the structural parameters extracted, do depend greatly on the tail fit. Hence great care should be taken when selecting channel limits for the tail fit. For realtime data it may be worthwhile to go through the dataset frame by frame, using the graphics option to check each fitted tail. It's also clear that the selection of the linear section of  $\Gamma_1$  in extract is yet to be perfected. While this is an annoying problem, it is not a vital aspect of the analysis programs since the user can always intervene. Extraction of structural parameters has concentrated on  $\Gamma_1$  up to the present. If possible, a program equivalent to extract will be written to analyse  $\Gamma_3$ . Future developments might include calculation of the interface distribution function from SAXS data and implication of the various methods for calculating degrees of crystallinity from WAXS data<sup>2</sup>.

### References.

1. Strobl, G. R.; Schneider, M. *J. Polym. Sci.* **1980**, 18, 1343-1359.
2. Baltá Calleja, F. J.; Vonk, C. G. *X-ray Scattering of Synthetic Poylmers*; Elsevier: Amsterdam, 1989; pp.247-251.
3. Baltá Calleja, F. J.; Vonk, C. G. *X-ray Scattering of Synthetic Poylmers*; Elsevier: Amsterdam, 1989; pp.257-261.
4. Koberstein, J.; Stein R. *J. Polym. Sci. Phys. Ed.* **1983**, 21, 2181-2200.
5. Press, W. H. et al. *Numerical Recipes: the Art of Scientific Computing*; Cambridge University Press, 1986.
6. Baltá Calleja, F. J.; Vonk, C. G. *X-ray Scattering of Synthetic Poylmers*; Elsevier: Amsterdam, 1989; pp.260-270.
7. Ryan, A.J.; Stanford, J.L.; Bras, W.; Nye, T.; *J. Polym. Sci . Phys .Ed.* submitted.

## EXTRACTING DATA FROM THE CORRELATION FUNCTION



## PROCESSING OF DNA HIGH-ANGLE FIBRE DIFFRACTION PATTERNS USING THE CCP13 SUITE

Lisa H.Simpson, Mark Shotton, and Trevor Forsyth

Physics Department, Keele University, Staffordshire ST5 5BG,  
U.K.

*The use of the CCP13 suite of programmes in the processing of high-angle x-ray diffraction data recorded from DNA fibres is described. Two examples have been chosen to demonstrate the application of these routines in the measurement of highly crystalline diffraction patterns. The first of these describes the processing of data recorded from the A conformation of a novel deaza derivative of the poly[d(A-T)].poly[d(A-T)] DNA double helix in which the N<sub>7</sub> position of adenine residues has been changed to a C-H group. The second example concerns the processing of fibre diffraction data which has recently been obtained from a thallium derivative of the D form of DNA.*

**Introduction** High-angle fibre diffraction is a powerful method in the analysis of DNA structure and in the investigation of conformational changes between DNA structures. Fibre diffraction studies of long polymeric DNA and also single crystal studies of oligonucleotide duplexes have provided clear evidence that water and cations in these systems occupy well defined locations which are crucial both to the stabilisation of each of the five principal forms of double-stranded DNA and to the mediation of conformational transitions which occur between these forms. This is well illustrated by time-resolved high-angle fibre diffraction studies of structural transitions in DNA which have been undertaken at the Daresbury SRS<sup>1,2,3</sup>. These observations have led to the use of x-ray isomorphous replacement methods in the study of the location of cations around DNA and to the application of isotopic replacement methods in complementary high-angle neutron fibre diffraction studies of DNA hydration<sup>4,5,6,7</sup>. Further insight into the factors which stabilise particular DNA conformations are being obtained from diffraction studies of chemically modified DNA in which particular base atoms are changed so that the relative importance of various DNA/ion/water interactions can be investigated in a very specific way. The first of the two examples described below concerns one such modification which is being used to probe the significance of major 'groove' interactions in stabilising particular DNA conformations.

These applications of fibre diffraction place heavy demands on data processing both from the point of view of the development of good algorithms and also in terms of the sheer volume of data that often requires processing. They have therefore benefitted enormously from the data measurement procedures currently available under CCP13 in which there has been a significant shift in emphasis away from interactive data processing methods. The development of these routines within a suite that is of wide application in fibre diffraction problems and which readily interfaces with other packages such as the CCP4 suite for protein crystallography and the BSL and OTOKO suites for non-crystalline diffraction is particularly important.

**Methods** All samples used for the work described here were made from DNA that was synthesised enzymatically for these studies. DNA synthesis was performed by incubation of the appropriate nucleoside triphosphates with DNA polymerase I in the presence of a DNA primer and magnesium chloride. Reaction mixtures were monitored by agarose gel electrophoresis and efficiencies measured using size exclusion chromatography. The final DNA product was purified and fibres drawn from concentrated gels using standard techniques.

Fibre diffraction data were recorded using the beamline 7.2 at the Daresbury SRS operating at a wavelength of 1.488Å obtained using the (111) plane of a germanium monochromator. This instrument has recently been refurbished and is now fully optimised for biological studies using high-angle fibre diffraction and protein crystallography. The fibre diffraction arrangement operates using a purpose-designed camera which allows the humidity of the sample environment to be closely controlled and monitored in a helium environment that eliminates scatter due to air. The system available on beamline 7.2 allows for data collection using photographic film, an online "Mar Research" image plate detector, or an offline "Molecular Dynamics" image plate system. A mount also exists which will accommodate a Photonic Science CCD detector on the optical bench.

Data were processed using firstly the routine CONV to convert the data-type to standard CCP13/BSL format. In the case of image plate data from the Molecular Dynamics system the routine SPD\_COR<sup>8</sup> was used prior to this to correct for spatial distortion effects. The interactive programme FLX was used to determine standard pattern parameters required for further processing. The data were then mapped into reciprocal space using FTOREC, and finally intensities measured using LSQINT. These procedures allowed the production of datasets that could then be readily fed into the CCP4 suite where a large number of programmes for the processing of single crystal data are available.

**The A form of Poly[d(c<sub>7</sub>A-T)].poly[d(c<sub>7</sub>A-T)]** This DNA polymer has been studied over a wide range of salt strengths and exhibits conformational polymorphism that is completely different from that observed for unmodified poly[d(A-T)].poly[d(A-T)]. It does not, in any circumstances yet identified, adopt the D conformation. In conditions which would normally favour the D form for the unmodified polymer it instead adopts an unusual variant of A-DNA and at very low humidities a novel conformation that has not been reported previously. Figure 1 shows a diffraction pattern recorded from the A form of this polymer. The molecule packs into a monoclinic lattice in space group C2 having parameters  $a=22.82\text{ \AA}$ ,  $b=40.67\text{ \AA}$ ,  $c=27.74\text{ \AA}$ ,  $\beta=96.7^\circ$ . The pattern exhibits clear differences in intensity distribution from that observed for classical A-DNA fibre diffraction patterns in the region of the 6th, 7th and 8th layer lines.

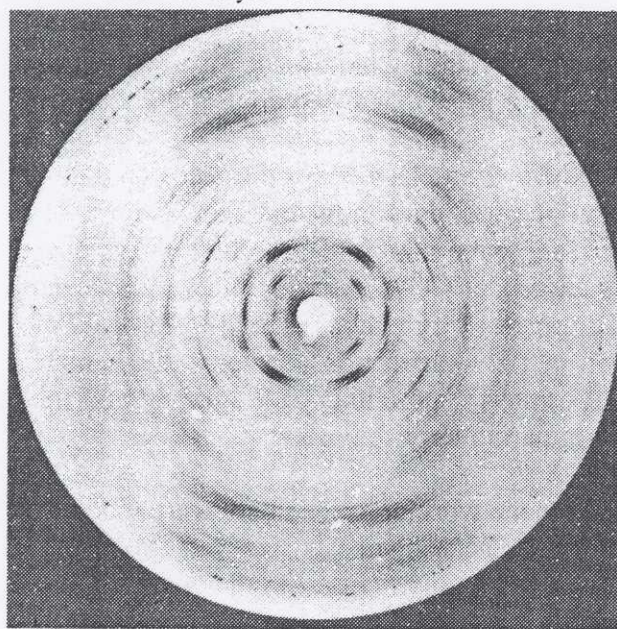


*Figure 1:* High-angle x-ray fibre diffraction pattern recorded from the A form of poly[d(c<sub>7</sub>A-T)].poly[d(c<sub>7</sub>A-T)]

Figure 2(a) shows the reciprocal space image produced from the data shown in Figure 1 using the routine FTOREC. The processing of FTOREC images using LSQINT requires reasonable starting values for the lattice parameters; these were obtained using FIX. The NOFIT option available within LSQINT was found to be particularly useful in estimating initial disorder parameters. The dataset shown in Figure 2(a) was measured by repeated applications of LSQINT using the maximum entropy (MAXENT) intensity fitting option available within the programme. Background was fitted to the pattern using the BACK WINDOW option. As with most A-DNA fibre diffraction patterns, data measurement was complicated by the effect of so-called "double orientation" which results in a slight displacement of some Bragg reflections either above or below the layer lines. This effect was well handled in LSQINT using the MISSETTING option which allowed a missetting angle to be refined alongside other parameters. The final fit to the observed data is seen in Figure 2(b) which shows a simulation of the pattern based on the fitted intensities. The agreement residual comparing the observed and the simulated data was 21%. The intensities measured from this pattern are currently being used to undertake a linked atom least squares (LALS<sup>9</sup>) analysis of this A-DNA helix.



*Figure 2:* (a) the FTOREC image obtained from the raw data shown in Figure 1; (b) an image simulated from the data measured by LSQINT.

**The Thallium salt of the D-DNA Double Helix** High-angle x-ray fibre diffraction patterns have recently been recorded from a thallium salt of the D-DNA double helix. The scattering power of the Tl<sup>+</sup> ( $Z=81$ ) cation in this derivative is markedly larger than was obtained in previous studies where difference Fourier methods based on data recorded from the Li<sup>+</sup>, Na<sup>+</sup>, K<sup>+</sup>, and Rb<sup>+</sup> salts of D-DNA were used to image cation locations around previously refined models for the DNA<sup>10,11</sup>. A thallium D-DNA diffraction pattern is shown in Figure 3. The D-DNA molecules form a centred orthorhombic array in space group C222<sub>1</sub> with lattice parameters  $a=23.45\text{\AA}$ ,  $b=25.32\text{\AA}$ ,  $c=24.30\text{\AA}$ . The distribution of intensity throughout the pattern is dramatically different from that recorded for other derivatives of D-DNA.

*Figure 3:* High-angle x-ray fibre diffraction pattern recorded from the thallium salt of D-DNA.

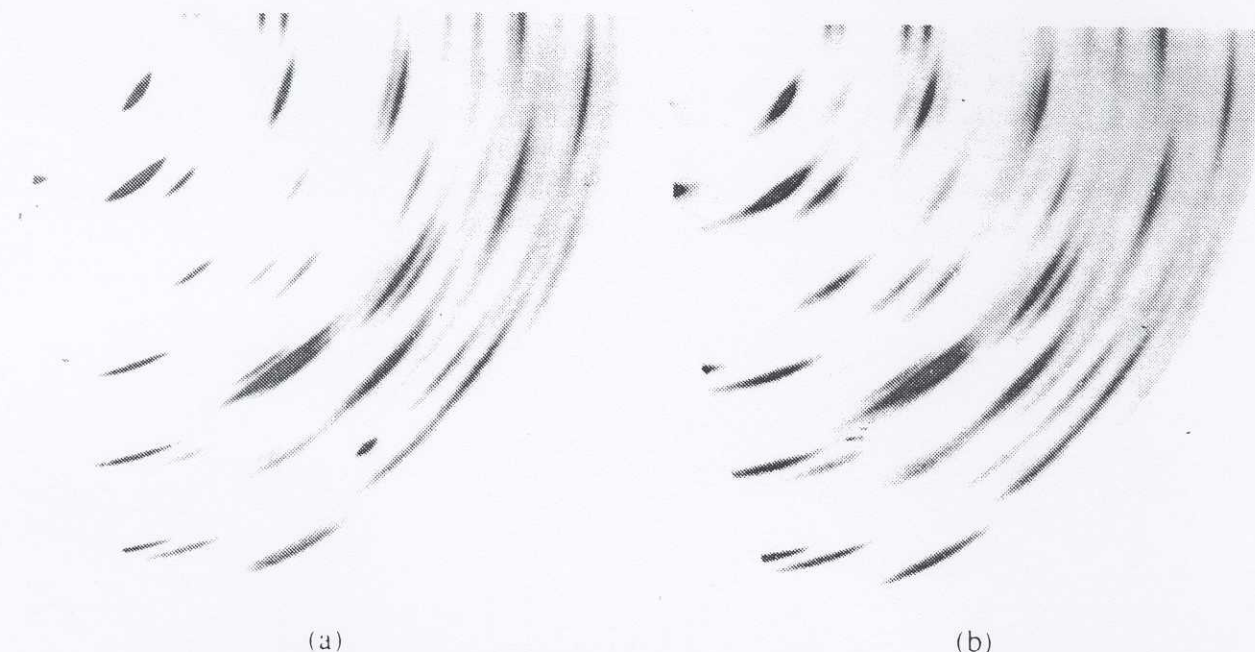
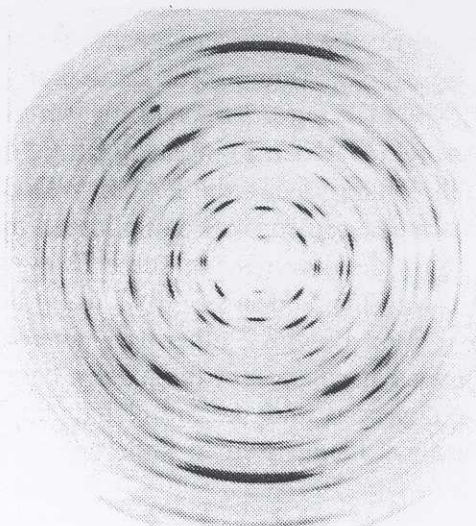


*Figure 4:* (a) the FTOREC image obtained from the raw data shown in Figure 3; (b) an image simulated from the data measured by LSQINT.

Figure 4(a) shows the reciprocal space image of this pattern as produced by FTOREC. The processing of this dataset with LSQINT followed essentially the same path as described for the previous example. However in this case the least-squares option of intensity fitting was used rather than the maximum entropy option. It was also found that in this case better results were obtained using the GLOBAL background fitting option. The final agreement residual was 24%. A Patterson analysis of this data is currently in progress.

**Conclusion** The examples described above demonstrate the efficacy of the programmes available within CCP13. It is clear that the resulting improvements in the accuracy with which data can be measured using these routines will have a major impact on the quality of fibre diffraction analyses

both for definitive structural work on "static" DNA conformations and also for the mapping of the stereochemical pathways followed during structural transitions using time-resolved high-angle x-ray fibre diffraction. The development and rationalisation of fibre diffraction software within CCP13 is being paralleled by a number of experimental developments which are occurring for x-ray and also for neutron high-angle fibre diffraction work at central facilities such as the Daresbury Laboratory SRS, the Institut Laue-Langevin reactor neutron source, and the ISIS spallation neutron source. The use of these facilities for fibre diffraction has a wide range of implications for data processing methods and it can be expected that CCP13 will provide an important framework within which such methods can be developed.

**Acknowledgements** We gratefully acknowledge support from the BBSRC and DRAL for the provision of beamtime on line 7.2. Particular thanks are also due to Richard Denny for help with the use of CCP13 routines, and to Dean Myles and Trevor Greenough for assistance with the instrumentation on beamline 7.2. The development of the fibre diffraction facilities now available of beamline 7.2 also owes much to the efforts of staff in the Keele University Physics Department workshop and we thank in particular Ted Greasely, Geoff Dudley, Derek James, and Graham Marsh. We also thank Mike Wallace and Mike Davis for general assistance which has been crucial to the success of these experiments, Helen Moors for secretarial assistance and Mike Daniels for the preparation of photographs.

### References

1. Mahendrasingam, A., Forsyth, V.T., Hussain, R., Greenall, R.J., Pigram, W.J., Fuller, W., *Science* 233, 133 (1986).
2. Forsyth, V.T., Greenall, R.J., Hussain, R., Mahendrasingam, A., Nave, C., Pigram, W.J., and Fuller, W., *Biochem. Soc. Trans.* 14, 533 (1986).
3. Mahendrasingam, A., Denny, R.C., Forsyth, V.T., Greenall, R.J., Pigram, W.J., Papiz, M.Z., and Fuller, W., *Inst. Phys. Conf. Ser.* 101, 225 (1989).
4. Forsyth, V.T., Mahendrasingam, A., Langan, P., Pigram, W.J., Stevens, E.D., Al-Hayalee, Y.A., Bellamy, K.A., Greenall, R.J., Mason, S.A., and Fuller, W., *Int. J. Biol. Macr.* 11, 236, (1989).
5. Fuller, W., Forsyth, V.T., Mahendrasingam, A., Pigram, W.J., Greenall, R.J., Langan, P., Bellamy, K.A., Al-Hayalee, Y.A., and Mason, S.A., *Physica B* 156/157, 468 (1989).
6. Langan, P., Forsyth, V.T., Mahendrasingam, A., Pigram, W.J., Mason, S.A., and Fuller, W., *J. Biomol. Str. Dyn.* 10(3), 489 (1992).
7. Langan, P., Forsyth, V.T., Mahendrasingam, A., Alexeev, D., Fuller, W., and Mason, S.A. *Physica B* 180/181, 759 (1992).
8. Hammersley, A.P., Svensson, S.O., Thompson, A., *Nucl. Inst. Meth.* A346, 312 (1994).
9. Smith, P.J.C., and Arnott, S., *Acta Cryst.* A34, 3 (1978).
10. Forsyth, V.T., Mahendrasingam, A., Langan, P., Pigram, W.J., Stevens, E.D., Al-Hayalee, Y.A., Bellamy, K.A., Greenall, R.J., Greenall, R.J., Mason, S.A., and Fuller, W., *Inst. Phys. Conf. Ser.* 101, 237 (1989).
11. Forsyth, V.T., Langan, P., Mahendrasingam, A., Mason, S.A., and Fuller, W., *Proc. Ital. Phys. Soc.* 43, 231 (1993).

---

# THE 1995 ACA MEETING

***MONTRÉAL, CANADA***

***July 23-28, 1995***

***Why not go to the SIG Session  
on  
FIBRE DIFFRACTION***

Contact: Y. LePage, Program Chair, NRC of Canada,  
Chem. Dept., Ottawa, Ontario K1A OR6, Canada.  
Tel: 613-993-2527; FAX: 613-952-1275.

---

---

# 1995 CCP13/NCD WORKSHOP

---

## "Diffraction from Fibres and Polymers"

This Workshop will be held at Daresbury Laboratory on May 9-11, 1995. It is an extended Workshop to allow full discussion of Fibre Diffraction and Non-Crystalline Diffraction results from natural and synthetic polymers.

The Provisional Timetable is as follows:

### Tuesday 9th May

11.00am	CCP13 Steering Committee meeting.
1.00pm	LUNCH
2.00 - 6.00pm	SESSION I: Synthetic Polymers
6.30pm	DINNER at Daresbury Laboratory
8.00 - 10.00pm	Wine mixer/ Poster Session/ Commercial Exhibition.

### Wednesday 10th May

9.00 - 1.00pm	SESSION II: Hardware - Sources and Detectors
1.00pm	LUNCH and POSTER VIEWING
2.00 - 5.00pm	SESSION III: Software Development
5.00 - 5.30pm	Quick-fire Poster Talks (max 2 minutes each!)
5.30 - 6.00pm	CCP13 General Business Meeting & Poster Prize Award
7.30pm	DINNER at the LORD DARESBURY HOTEL

### Thursday 11th May

9.00 - 1.00pm	SESSION IV: Biological Systems
1.00pm	LUNCH
2.00 - 4.00pm	SESSION V: Biological Systems (continued)
4.00pm	TEA and CLOSE of MEETING

Note that it is hoped that each Session will be opened with a 'Plenary' Lecture by an eminent scientist, some of whom will be from overseas.

---

## NOTES ON THE 1995 CCP13/NCD WORKSHOP

---

REGISTRATION FORMS for the Workshop will be sent by separate mailing to those on the CCP13 mailing list and to all NCD Daresbury users. Please apply to the Conference Office at Daresbury for a form if you are not on either mailing list.

ABSTRACTS, which should be legible at half A4 size, will be published in the 1995 edition of this Newsletter if signed at the May 1995 Workshop.

Deadline for receipt of Abstracts: March 31st, 1995

Deadline for registration: March 31st, 1995

ABSTRACT FORMAT: Half a side of A4 suitable for direct copying, including a clear title in Capitals and on the next line all authors and their addresses. Use single line spacing and 10 or 12 point type. Any Figures that need to be in the Abstract should lie within the half A4 area.

---

POSTER PRIZES will be awarded for the two Posters that the Judges like best; first prize £100, second prize £50. The judges will be selected from the distinguished speakers from overseas. Remember when making posters: to keep the wording to a minimum, not to try to say everything but to select a 'take home message' that you want the viewer to go away with, to keep the poster simple, to keep the lettering very large. You will be asked to stand by your poster for part of the Tuesday evening 'Poster Session'. In the Wednesday afternoon session there will also be time for you to give a TWO minute (2 slide or overhead) summary of your Poster to generate people's interest in your work.

---

BURSARIES will be available for a number of students and young scientists to attend the meeting. Please apply to the Conference Office at Daresbury with a legible Abstract, a reason for requesting support, and (in the case of students) the signed approval of your supervisor. Sponsored students and young scientists will be required to bring a Poster and to supply an Abstract.

---

For further details of the meeting please contact THE CONFERENCE & EVENTS OFFICE, Daresbury Laboratory, Warrington, Cheshire WA4 4AD.  
(Tel: 0925 603235. Fax: 0925 603195)

---

---

# 1995 CCP13/NCD WORKSHOP

---

## "Diffraction from Fibres and Polymers"

**Tuesday 9th to Thursday 11th, May 1995  
DARESBURY LABORATORY**

Following the success of the first three Fibre Diffraction Workshops at Daresbury, the Fourth Workshop is being organised at the Daresbury Laboratory by CCP13 in Fibre Diffraction and the Non-Crystalline Diffraction (NCD) User community at Daresbury. Application details are given in this Newsletter. Those on the CCP13 or NCD mailing lists will automatically be sent application forms. Others can apply directly to the Conference Office, Daresbury Laboratory, Warrington, Cheshire WA4 4AD.

It is very much hoped that you and your colleagues will be able to come to this meeting so that the CCP and NCD groups get full input from interested users. As before, the Workshop will consist of a healthy mix of technical and hardware discussion, software reports and presentations of recent results. Abstracts will be published in the 1995 edition of this Newsletter.

### ***INVITED SPEAKERS INCLUDE***

*Gerhard Zachmann  
Lee Makowski      Don Marvin,  
                        Harry Reynaers*

For further details of the meeting please contact THE CONFERENCE & EVENTS OFFICE, Daresbury Laboratory, Warrington, Cheshire WA4 4AD. (Tel: 0925 603235. Fax: 0925 603195)

---